Received: 14 May 2020 | Revised: 18 September 2020 | Accepted: 18 October 2020
DOI: 10.1002/ar.24567

SPECIAL ISSUE ARTICLE

The Anatomical Record
Advances in Integrative Anatomy and Evolutionary Biology
WILEY

Paleoneurology of *Baurusuchus* (Crocodyliformes: Baurusuchidae), ontogenetic variation, brain size, and sensorial implications

Marcos V. Dumont Jr[1,2] | **Rodrigo M. Santucci**[2] | **Marco Brandalise de Andrade**[3] | **Carlos Eduardo Maia de Oliveira**[4]

[1]Federal Institute of Brasília, Brasília, Brazil
[2]University of Brasília, Brasília, Brazil
[3]Pontifical Catholic University of Rio Grande do Sul, PUCRS, School of Health and Life Sciences, Porto Alegre, Brazil
[4]Federal Institute of Education, Science and Technology of São Paulo, Votuporanga, Brazil

Correspondence
Marcos V. Dumont Jr, Federal Institute of Brasília, Campus Planaltina, Brasília, DF, Brazil.
Email: dumont.marcos@gmail.com

Funding information
Conselho Nacional de Desenvolvimento Científico e Tecnológico, Grant/Award Number: 401784/2010-0

Abstract

Knowledge on crocodyliform paleoneurology has significantly improved with development of computed tomography. However, studies so far have been able to reconstruct brain endocasts based only on single specimens for each taxon. Here for the first time, we reconstructed brain endocasts for multiple fossil specimens of the same crocodyliform taxon (*Baurusuchus*), consisting of complete skulls of two medium sized specimens, one large adult, and a late juvenile. In addition, we were able to reconstruct the inner ear anatomy of a fragmentary skull using microtomography. We present estimates of brain size using simple models, based on modern Crocodylia, able to adapt brain to endocranial cavity ratios to expected ontogenetic variation instead of using fixed ratios. We also analyzed relative brain sizes, olfactory ratios, facial sensation, alert head posture, best hearing frequencies, and hearing range. The calculated endocranial volumes showed that they can be greatly altered by taphonomic processes, altering both total and partial endocranial volumes. Reconstructed endocasts are compatible with different degrees of occupation along the endocranial cavity and some of their characteristics might be useful as phylogenetic characters. The relative brain size of *Baurusuchus* seems to be small in comparison to modern crocodilians. Sensorial abilities were somewhat similar to modern crocodilians and hearing ranges and best mean frequencies remarkably similar to modern taxa, whereas olfactory ratio values are a little higher. Differing from its modern relatives, *Baurusuchus* hypothesized alert head posture is compatible with a terrestrial habit.

KEYWORDS
Baurusuchus, brain, endocast, nerves, ontogeny, paleoneurology

1 | INTRODUCTION

Paleoneurology is the study of the nervous systems of fossil organisms (Buchholtz & Seyfarth, 1999; Edinger, 1938; Hopson, 1979) and provides insight on vertebrate evolution and paleoecology (e.g., George & Holliday, 2013; Hurlburt, Ridgely, & Witmer, 2013; Walsh, Barrett, Milner, Manley, & Witmer, 2009; Witmer, Ridgely, Dufeau, & Semones, 2008; Zelenitsky, Therrien, & Kobayashi, 2009; Zelenitsky, Therrien, Ridgely, McGee, & Witmer, 2011). In extinct vertebrates, evidence for behavior comes mainly from comparative osteology (Walsh & Knoll, 2011). In this sense, paleoneurology is an independent line of evidence for behavior that yields information that osteology alone fails to reveal, such as sensory and cognitive abilities (George & Holliday, 2013; Hoffmann, Rodrigues, Soares, & Andrade, 2019; Hurlburt et al., 2013; Walsh et al., 2009; Witmer et al., 2008; Zelenitsky et al., 2009, 2011).

For much of its history, paleoneurology was dependent on either fortuitous findings or potentially destructive methods (Buchholtz & Seyfarth, 1999; Edinger, 1938, 1941, 1975; Edinger, 1975; Gaffney, 1977; Galton, 1989, 2001; Hopson, 1979; Jerison, 1973; Newton, 1888; Osborn, 1912; Radinsky, 1968; Stensiö, 1963). Recently, technological advances in computed tomography (CT) scanning have fomented a huge increase in paleoneurological knowledge. For instance, pre-CT technology studies of crocodyliform paleoneurology are scarce (e.g., Colbert, 1946; Edinger, 1938) in comparison to studies based on CT scans (e.g., Blanco et al., 2015; Bona, Carabajal, & Gasparini, 2017; Bona, Degrange, & Fernández, 2013; Brusatte et al., 2016; Fernández, Carabajal, Gasparini, & Chong, 2011; Fonseca et al., 2020; George & Holliday, 2013; Herrera, Fernández, & Gasparini, 2013; Holliday & Gardner, 2012; Kley et al., 2010; Pierce, Williams, & Benson, 2017; Serrano-Martínez, Knoll, Narváez, Lautenschlager, & Ortega, 2019; Sertich & O'Connor, 2014; Tykoski, Rowe, Ketcham, & Colbert, 2002). These recent studies led to a great advance in crocodyliform paleoneurological knowledge. However, these studies still represent only a small fraction of known crocodyliform taxa (Serrano-Martínez et al., 2019).

Despite the advances regarding crocodyliform paleoneurology, some important investigations are yet to be conducted. Probably, mainly due to the nature of the fossil record, paleoneurological evidence in the literature for any crocodyliform taxa is based on single specimens (e.g., Blanco et al., 2015; Bona et al., 2013; Bona et al., 2017; Brusatte et al., 2016; Colbert, 1946; Edinger, 1938; Fernández et al., 2011; Fonseca et al., 2020; George & Holliday, 2013; Herrera et al., 2013; Holliday & Gardner, 2012; Kley et al., 2010; Pierce et al., 2017; Serrano-Martínez et al., 2019; Sertich & O'Connor, 2014; Tykoski et al., 2002). This impairs our capacity to understand both the effects of deformation in retrieved endocast volumes, ontogenetic variation regarding brain size and shape, and intraspecific variability.

Fossil crocodyliforms are common in Adamantina Formation deposits, especially baurusuchids, represented by well-preserved cranial and postcranial materials (Montefeltro, Larsson, & Langer, 2011; Nascimento & Zaher, 2011; Price, 1945; Riff & Kellner, 2001; Vasconcellos & Carvalho, 2007; Vasconcellos, Marinho, & Carvalho, 2007). The Upper Cretaceous Adamantina Formation (Bauru Group) crops out in central and Southern regions of Brazil (Fernandes & Coimbra, 2017). There is no consensus regarding the stratigraphic division of the Bauru Group (Dias-Brito, Musacchio, Castro, Maranhão, & Suárez, 2001; Fernandes & Coimbra, 1996; Milani & Zalan, 1999; Soares, Landim, Fúlfaro, & Neto, 1980) and this also holds true for the Adamantina Formation. Some authors divide it into Vale do Rio do Peixe, São José do Rio Preto, and Presidente Prudente formations due to regional variations (Fernandes, 1998; Fernandes & Coimbra, 2017). However, we use the original designation (Adamantina Formation), described by other works that take into account lithologic variations as a typical characteristic of the unit (Batezelli, 2003; Garcia, Da Rosa, & Goldberg, 2005; Silva, 2003). There is a dispute between a Campanian-Maastrichtian and Turonian-Santonian age for the Adamantina Formation (Dias-Brito et al., 2001; Gobbo-Rodrigues, Petri, & Bertini, 1999; Santucci & Bertini, 2001). However, accumulated evidences so far seem to give better support for the Campanian-Maastrichtian age (Batezelli, 2017; Batezelli, Saad, de Jesús Perinotto, Fulfaro, & Etchebehere, 2003; Castro et al., 2018; Granot, Dyment, & Gallet, 2012; Tamrat et al., 2002).

Baurusuchus Price, 1945, from the Adamantina Formation, is the type genus of the Baurusuchidae Price, 1945. This is a group of medium to large-sized, terrestrial, predatory crocodyliforms from the Cretaceous of South America and possibly Pakistan. They have tall, laterally compressed skulls and reduced number of teeth, which are serrated and, some of them, hypertrophied (Carvalho, Gasparini, Salgado, Vasconcellos, & Marinho, 2010; Montefeltro et al., 2011; Nascimento & Zaher, 2011; Price, 1945; Riff & Kellner, 2001; Vasconcellos et al., 2007; Vasconcellos & Carvalho, 2007). Their phylogenetic relations are still disputed; the Pakistani species *Pabwehshi pakistanensis* Wilson, Malkani, & Gingerich, 2001 is included in the family by some cladograms (Nascimento & Zaher, 2011; Pol & Powell, 2011; Turner & Calvo, 2005) but excluded in other (Larsson & Sues, 2007). Baurusuchids were cursorial predators with a series of convergences with carnivorous theropod dinosaurs, being among the top predators of South American Late Cretaceous faunas (Godoy, Montefeltro, Norell, & Langer, 2014; Price, 1945; Riff & Kellner, 2001, 2011; Vasconcellos & Carvalho, 2007).

Although there are works regarding *Baurusuchus* anatomy and paleoecology, none of them describe its neuroanatomy (Carvalho et al., 2010; Riff & Kellner, 2001; Vasconcellos et al., 2007; Vasconcellos & Carvalho, 2007). Despite being an important component of Brazilian Cretaceous fauna, knowledge on Baurusuchidae neuroanatomy is still scarce. The only work on baurusuchid neuroanatomy so far is Fonseca et al. (2020) on *Campinasuchus dinizi* Carvalho et al., 2011, from the Adamantina Formation, Brazil. Despite being able to reconstruct endocranial endocast and head sinuses, they did not provide any information on the cranial nerves. In addition, their reconstructed inner ear is incomplete due to poor preservation.

The relative abundance of *Baurusuchus* skull materials makes it possible to study its neuroanatomy, as well as factors that can influence reconstructed neuroanatomy in fossil taxa, such as deformation and ontogenetic stage. In living crocodyliforms, the central nervous system grows continually, with the endocranial cavity growing faster than the brain, making brain to endocast ratios and morphological correspondence vary even among adult individuals of different sizes (Hurlburt et al., 2013; Jirak & Janacek, 2017; Ngwenya et al., 2013; Watanabe et al., 2019). In this sense, our study aims to describe *Baurusuchus* neuroanatomy in detail using CT scans from specimens of different ontogenetic stages, with different deformation degrees, discussing variation among specimens. Based on reconstructed neuroanatomy, we discuss the relative brain size and sensorial implications for olfaction, alert head posture, hearing, and facial sensitivity.

1.1 | Anatomical abbreviations

For nomenclature of anatomical features, we follow Witmer et al. (2008) and Iordansky (1973). Anatomical abbreviations—**blty**, tympanic bulla; **c**, cochlea; **car**, cerebral carotid artery canal; **cer**, cerebral hemisphere; **crc**, crus communis; **csc**, caudal (posterior vertical) semicircular canal; **dc**, dorsal contour; **dls**, dorsal longitudinal sinus; **eo**, exoccipital; **fc**, fenestra cochleae (= round window); **fv**, fenestra vestibuli (= oval window); **II–XII**, cranial nerve canal number; **lsc**, lateral (horizontal) semicircular canal; **ob**, olfactory bulb; **ot**, olfactory tract; **p**, parietal; **pit**, pituitary (= hypophyseal) gland; **pot**, prootic; **rsc**, rostral (anterior vertical) semicircular canal; **rsca**, ampulla of rostral semicircular canal; **so**, supraoccipital; **V1**, ophthalmic nerve canal; **V2–3**, maxillomandibular nerve canal; **V2-so**, canal for supraorbital branch of maxillary nerve; **Vgang**, trigeminal (Gasserian) ganglion; **vls**, ventral longitudinal sinus; **Vtym**, tympanic branch of trigeminal nerve canal; **VIIIcoch**, cochlear branch of vestibulocochlear nerve canal.

1.2 | Institutional abbreviations

FEF-PV, Fernandópolis Educational Foundation, São Paulo; **FUP**, University of Brasília, campus Planaltina, Federal District; **IFSP-VTP**, Federal Institute of Education, Science and Technology of São Paulo (Votuporanga, São Paulo, Brazil).

2 | MATERIALS AND METHODS

2.1 | Fossil specimens

Five fossil specimens attributed to the genus *Baurusuchus* were used in this study (Figure 1), all collected from deposits of the Adamantina Formation in São Paulo State, in the cities of Fernandópolis and Jales. Specimen IFSP-VTP/PALEO-0003 is an almost complete late juvenile individual, lacking the entire tail, except for the first two caudal vertebrae and their respective haemal arches, from Fernandópolis, found in dorsoventral position, with the skull roof slightly damaged. In IFSP-VTP/PALEO-0003 the neural arches and vertebral centra are incompletely fused, and dermal plates are very thin, indicating the earlier ontogenetic stage. All other specimens are adult individuals, represented only by their skulls and partial postcrania. The specimen IFSP-VTP/PALEO-0002, from Fernandópolis, was found in dorsoventral position and is considerably deformed dorsoventrally. Specimens FUP-Pv 000020 (complete skull without mandible) and FEF-PV-R-1/9 (complete skull with mandible and part of postcranium) were found in Jales laying in lateral position and are slightly laterally deformed. All complete skulls, including the late juvenile, share synapomorphies for the genus, the jugal antorbital region is more expanded than the infraorbital, major surface of pterygoid wing is latero-ventrally oriented and the surangular-angular lateral surface has a marked depression for insertion of musculus pterygoideous posterior (Montefeltro et al., 2011). Specimen FUP-Pv 000021 (found few meters apart from the specimen FEF-PV-R-1/9) is a fragmentary skull from Jales comprising the right otic capsule and fragments of adjacent bones and, as far as comparisons can be made, with features identical to the other studied specimens.

2.2 | CT scan

All specimens were mechanically prepared before image acquisition. The specimen FEF-PV-R-1/9 was scanned in a CT scan model Biograph 16 Siemens kV in Santa Casa de Votuporanga-SP, resulting in 600 slices of 0.75 mm

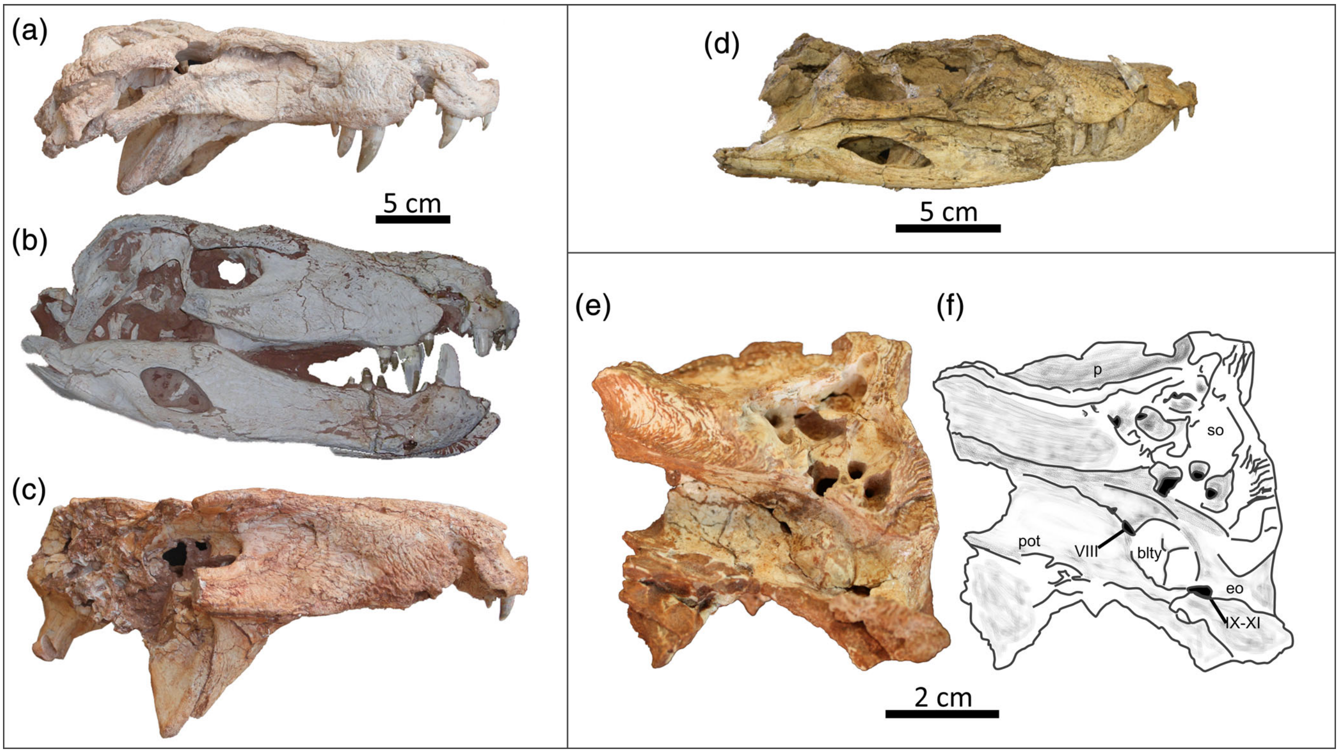

FIGURE 1 Specimens used in this study. Adult skulls right lateral views IFSP-VTP/PALEO-0002 (a), FEF-PV-R-1/9 (b), FUP-Pv 000020 (c); late juvenile skull right lateral view IFSP-VTP/PALEO-0003 (d); fragmentary skull left medial view FUP-Pv 000021 (e,f). btly, tympanic bulla; eo, exoccipital; p, parietal; pot, prootic; so, supraoccipital; VIII–IX, cranial nerve canal number. Scale bars a–d: 5 cm; e,f: 2 cm

each, with resolution of 768 × 768 pixels, 120 kV, and 200 mA. Specimens IFSP-VTP/PALEO-0003, IFSP-VTP/PALEO-0002, and FUP-Pv 000020 were scanned in a CT scan model Revolution EVO in IMEB (Imagens Médicas de Brasília-DF) resulting in 392, 593, and 692 slices, respectively of 0.50 mm each, with resolution of 512 × 512 pixels, 140 kV, and 240 mA. Specimen FUP-Pv 000021 was scanned in a microCT scanner model Skyscan1076, in Laboratório de Nanobiotecnologia, Instituto de Biologia from University of Brasília, which provided 2,640 slices, with a pixel resolution of 9.0 μm, 100 kV, and 100 μA. Three-dimensional reconstructions and segmentations were made in the free software InVesalius (Amorim, de Moraes, Azevedo, & da Silva, 2011). Segmentation was made by manual thresholding and three-dimensional surfaces were generated using the context aware smoothing algorithm.

2.3 | Analysis

2.3.1 | Calculating body and brain mass

Estimates of body mass for fossil mesoeucrocodylians are typically done using linear measurements, such as skull and femur length, and body mass linear regression equations of living Mesoeucrocodylia (Cotts, Pinheiro, Marinho, Carvalho, & Di Dario, 2017; Farlow, Hurlburt, Elsey, Britton, & Langston Jr, 2005). Our materials consist mostly of isolated skulls, making skull measurements a better choice. The different degrees in lateral compression preclude the use of skull width measurements as suggested by O'Brien et al. (2019). The largest adult specimen skull length is 14% larger than the smallest adult skull, but the smallest adult skull width is 24% wider than the largest one. Therefore, body masses were estimated using the regression equation relating skull length (SL) and body mass (MBr) for modern Crocodylia: $\log \mathrm{MBd} = (\log \mathrm{SL} \times 3.48)\text{—}6.97$ in Farlow et al. (2005), obtained by direct measurement of both skull length and body masses for a series of *Alligator mississippiensis* individuals.

Cranial endocasts can be used to accurately estimate brain size in both birds and mammals because their brains fill the endocranial space almost completely, differing from other vertebrate groups (Currie, 1995; Larsson, Sereno, & Wilson, 2000). Initially, reptile brains were thought to occupy about 50% of endocranial volume, based on *Sphenodon* and *Iguana* specimens (Dendy, 1910; Jerison, 1973). More recently, it has been shown that this occupation ratio is more complex, varying not only among species, but also throughout ontogeny (Hurlburt et al., 2013; Jirak & Janacek, 2017; Watanabe et al., 2019).

In crocodilians, brain and endocast volumes are highly correlated if proper estimation is applied (Hurlburt et al., 2013; Jirak & Janacek, 2017; Watanabe et al., 2019). In other words, endocranial volumes are a proxy of brain size, but approaches that uses constant brain to endocast ratios are likely to return inaccurate results. This is because the ratio of brain occupation varies from nearly 100% in embryos and hatchlings, to about 67% in small adults to 30% in large adults of larger species (e.g., *Alligator mississippiensis*, *Crocodylus niloticus*). In nonavian Archosauriformes this problem has been addressed by obtaining brain size estimates with more than one ratio, typically 37 and 50% unless there is evidence of higher brain occupancy (e.g., Hurlburt et al., 2013; Lauters, Vercauteren, Bolotsky, & Godefroit, 2013; Paulina-Carabajal & Currie, 2017; Trotteyn & Paulina-Carabajal, 2016). This kind of approach narrows the possibilities for estimated brain mass, but still gives a large range of possible values. More recently, Serrano-Martínez et al. (2019) used data from living Crocodylia to obtain a regression formula relating endocranial and brain volumes as a more appropriate method to deal with the varying brain to endocranial ratio. In this sense, we estimated brain masses using two separate approaches: linear regression and partial brain volumes from model organisms. Since the specific gravity of the brain is close to 1.0 (Jerison, 1973), we consider calculated brain volumes in ml to be equivalent to brain masses in g.

For the linear equation, crocodilian brain and endocranial volumes were gathered from the literature (Hurlburt et al., 2013; Jirak & Janacek, 2017; Watanabe et al., 2019) and subsequently log transformed and plotted in the software PAST (Hammer, Harper, & Ryan, 2001), where an ordinary least-squares (OLS) regression was performed for two datasets: one containing only *Alligator mississippiensis* and the other containing all crocodilian data. We also ran a phylogenetic generalized least-squares regression (PGLS; Freckleton, Harvey, & Pagel, 2002; Grafen, 1989; Martins & Hansen, 1997; Pagel, 1997, 1999; Rohlf, 2001) implemented in RStudio (RStudio Team, 2020) for the data containing more than one species in order to estimate phylogenetic signal influence. Cladograms were obtained from Oaks (2011), Pol et al. (2014), Groh, Upchurch, Barrett, and Day (2020) and merged for construction of a larger and more detailed cladogram. Tree calibration used timePaleoPhy (Bapst, 2012, 2013) package with bin_ timePaleoPhy routine to account for the temporal uncertainty among fossil species. Fossil species chronostratigraphic intervals were transformed into age ranges (in Ma) according to the latest updated version of the Chronostratigraphic International Chart (Cohen, Finney, Gibbard, & Fan, 2013 updated), 2020/01 version. The function minimum branch length (MBL) was used in order to avoid creating zero-length branches when calibrating the trees. Twenty different calibrated trees were generated to check for effects of the stratigraphic range attributed to fossil taxa in the analysis. After calibration, trees were pruned to keep only the taxa with available brain and endocranial volumes. Multiple specimens from the same species were included in the cladogram as a polytomy (Felsenstein, 2008; Liberona, Soto-Acuña, Mendez, & Vargas, 2019) to account for intraspecific variation. The λ parameter, under Brownian motion was used to define strength of phylogenetic influence (Pagel, 1999), adjusted automatically according to a maximum likelihood function. Best data fit between OLS and PGLS functions was defined using the Akaike Information Criterion (Akaike, 1973).

For the partial brain volumes approach, we divided each endocast in four major areas: olfactory (olf), prosencephalic (pros), mesencephalic (mes), and rhombencephalic (rhomb), based on Jirak and Janacek (2017). Limits between adjacent areas are endocast based, being less precise than brain based areas, which are only possible for living specimens. We used cerebral hemisphere anterior and posterior limits as landmarks to differentiate olf-pros and pros-mes limits, and the widest point of the cerebellar region to define mes-rhomb limit. A living individual of similar endocranial volume, or two living individuals in which the endocranial volumes range overlaps fossil specimen endocranial volume were chosen as a model from published partial volumes data (Jirak & Janacek, 2017). Then, partial brain to endocast ratio in the living organisms were used to estimate fossil specimens brain size. When two living individuals were used, the brain volume was calculated in each and presented as an average. Partial endocranial volumes were also measured and compared with modern crocodilians (Jirak & Janacek, 2017).

In vertebrates, brain and body size are highly correlated, where the brain tends to be relatively smaller in large-bodied taxa (Hurlburt et al., 2013). Relative brain size has been used to infer cognition and thermoregulatory mechanisms of extinct vertebrates based on living vertebrate species (Hopson, 1977; Jerison, 1973; Lefebvre, Nicolakakis, & Boire, 2002; Marino, 2002). Traditionally, observed brain size is divided by an expected brain size for a given body mass using regression equations for the appropriate vertebrate group (Hurlburt, 1996; Hurlburt et al., 2013; Jerison, 1973). This approach is known as encephalization quotient, and the group used to calculate expected brain mass is represented in front of the name (e.g., reptile encephalization quotient standard (REQ), bird encephalization quotient standard, and so on (Hurlburt, 1996; Hurlbert et al., 2013; Jerison, 1973)). Unfortunately, the use of REQs is problematic when studying modern Mesoeucrocodylia, since their REQs decrease throughout ontogeny even when only adult individuals are taken into account (Hurlburt et al., 2013). However, brain and body mass data for living crocodilians is available in the literature for a few taxa (e.g., Chentanez, Huggins, & Chentanez, 1983; Crile & Quiring, 1940; Gans, 1980; Hurlburt et al., 2013; Jirak & Janacek, 2017; Ngwenya et al., 2013; Platel, 1979), allowing direct comparisons.

2.3.2 | Olfaction and olfactory ratio

Olfactory bulbs are responsible for processing sensory input from the olfactory nerve (CN I), since the contact between odor particles and olfactory epithelium in the nasal cavity fires neurons that transmit the neural signal to the olfactory bulbs via CN I (Purves, Augustine, & Fitzpatrick, 2001; Vassar et al., 1994). The olfactory bulbs collect and process these stimuli and send signals to higher processing centers of the brain through the olfactory tract (Mori, Nagao, & Yoshihara, 1999; Purves et al., 2001). Relatively larger olfactory bulbs and wider variability of olfactory receptors are positively correlated, enabling detection of a larger array of odor molecules (Bang & Cobb, 1968; Buschhüter et al., 2008; Clark, Avilova, & Bean, 1993; Hammock, 2005; Healy & Guilford, 1990; Krebs, Sherry, Healy, Perry, & Vaccarino, 1989; Niimura & Nei, 2006; Nottebohm, Kasparian, & Pandazis, 1981; Purves et al., 2001; Steiger, Fidler, Valcu, & Kempenaers, 2008; Vassar et al., 1994; Wenzel & Meisami, 1987). Modern crocodilians have a keen sense of smell and large olfactory bulbs, using olfaction to navigate, locate food sources, and for intraspecific communication (Schwenk, 2008; Scott & Weldon, 1990; Weldon & Ferguson, 1993; Zelenitsky et al., 2009, 2011).

The olfactory ratio is a method of measuring the relative size of olfactory bulbs, widely employed for inferring olfactory capabilities in living and fossil archosaurs (Bang & Cobb, 1968; Cobb, 1960; Serrano-Martínez et al., 2019; Zelenitsky et al., 2009, 2011). The olfactory ratio is the quotient between the largest linear measurement of both olfactory bulb and cerebral hemispheres, regardless of orientation (Bang & Cobb, 1968; Cobb, 1960; Zelenitsky et al., 2009, 2011). Olfactory ratios are indicative of olfactory capability and have been associated with a series of ecological factors in birds (see Zelenitsky et al., 2009 and references therein). As expected for their keen sense of smell and large olfactory bulbs, crocodilians have high olfactory ratios (Serrano-Martínez et al., 2019; Zelenitsky et al., 2009). Since olfactory ratios and ecological factors are related, the values for all Crocodylia sampled so far might be similar due to their similar ecologies (Grigg & Kirshner, 2015).

2.3.3 | Inner ear, alert head posture, and hearing

In gnathostomates, the inner ear typically consists of two main components: the semicircular canals, sensing angular accelerations, and the cochlea (lagena) sensing mechanical waves (sound) (Baird, 1970; Spoor, 2003; Spoor et al., 2007; Spoor & Zonneveld, 1998). Since, the bones of the otic capsule encase both, their gross anatomy can be reconstructed even when only skeletal elements are available, such as in fossil vertebrates (Gleich, Dooling, & Manley, 2005; Walsh et al., 2009; Witmer et al., 2008).

There is a strong correlation between cochlear linear measurements with hearing range and mean hearing frequency (Manley, 1972; Walsh et al., 2009). Vocalization in vertebrates is generally produced within the species hearing range (Brown & Waser, 1984; Endler, 1992; Konishi, 1970; Narins et al., 2004) and its complexity is related to ecological factors such as sociability and gregarism (Blumstein & Armitage, 1997; Evans, 1936). In addition, species living in environments where visual communication is limited tend either to have vocalizations that are more complex or use lower frequencies than species living in open environments (Brown & Waser, 1984; Garrick & Lang, 1977). Best mean hearing frequencies and hearing ranges were estimated using log transformed endosseous cochlear duct length scaled to basicranial axis length (basioccipital plus basisphenoid) using respectively the equations: $y = 3{,}311.3x + 4{,}000.8$ and $y = 6{,}104.3x + 6{,}975.2$ from Walsh et al. (2009).

The orientation of the lateral semicircular canal is used in some studies as a proxy for the alert head posture (e.g., Witmer et al., 2008; Witmer, Chatterjee, Franzosa, & Rowe, 2003) based on literature covering mammals, birds, and crocodilians (e.g., Blanks, Curthoys, & Markham, 1972; Erichsen, Hodos, Evinger, Bessette, & Phillips, 1989; Witmer et al., 2008). However, other studies claim that lateral semicircular canal should not be used as a reference for alert head posture (e.g., Marugán-Lobón, Chiappe, & Farke, 2013; Taylor, Wedel, & Naish, 2009). Among the reasons, they point that semicircular canals tend to be misaligned with Earth's axes (Benoit, Farke, Neenan, & Manger, 2019; Graf, De Waele, & Vidal, 1995; Hullar, 2006; Spoor & Zonneveld, 1998). This misalignment is regarded as physiologically advantageous for vestibular reflexes, since the misalignment between the lateral semicircular canal (lsc) and the horizontal plane makes all three semicircular canals sensitive to horizontal acceleration, improving sensorial input (Cohen & Raphan, 2004). In addition, Duijm (1951) found highly variable inclination values between lsc and the horizontal plane for 33 bird species, despite the average inclination of all species being close to horizontal (0°) the inclination varied from 30° anterodorsally to 20° anteroventrally. Alternatively, these studies propose other proxies for inferring head alert posture such as aligning either the maxillary tooth row (Marugán-Lobón et al., 2013) or the endocranial surface of braincase and bony palate (Kley et al., 2010; von Baczko, Taborda, & Desojo, 2018) to the horizontal plane. Therefore, we used three different anatomical proxies for fossil vertebrates to infer alert head posture: the lateral semicircular canal (but see alert head posture in the discussions; Witmer et al., 2003, 2008), maxillary tooth row (Marugán-Lobón et al., 2013), and the endocranial surface of braincase and bony palate (Kley et al., 2010; von Baczko et al., 2018).

2.3.4 | Trigeminal fossa and facial sensitivity

In mesoeucrocodylians, the trigeminal nerve exits the endocranial cavity through the trigeminal foramen, formed by the laterosphenoid and the prootic (George & Holliday, 2013; Holliday & Witmer, 2009; Hopson, 1979). From the trigeminal foramen the nerve goes into the trigeminal fossa (Vfossa), surrounded medially by the laterosphenoid and prootic, and laterally by the pterygoid and quadrate, housing the trigeminal ganglion (Vgang; George & Holliday, 2013; Holliday & Witmer, 2009; Hopson, 1979). From the trigeminal ganglion, the trigeminal ophthalmic branch exits anteriorly via ophthalmic nerve foramen, perforating the laterosphenoid, whereas the trigeminal maxillary and mandibular branches exit together through the maxillomandibular foramen (mmf), bordered by the laterosphenoid, pterygoid, and quadrate (George & Holliday, 2013; Holliday & Witmer, 2009; Hopson, 1979). Living and fossil Crocodylia have relatively large Vfossa and mmf, whereas other mesoeucrocodylians have relatively small ones (George & Holliday, 2013; Holliday & Witmer, 2009; Hopson, 1979). The presence of a unique trigeminal-innervated, highly sensitive mechanoreceptive system in the crocodilian face (integumentary sensory organs—ISOs) is a possible reason for this Vgang enlargement (George & Holliday, 2013). This sensory system is important for the crocodilian semiaquatic lifestyle as it can detect pressure changes in the surrounding water (Di-Poï & Milinkovitch, 2013; Grap, Machts, Essert, & Bleckmann, 2020; Leitch & Catania, 2012; Soares, 2002; von During, 1973; von During, 1974; von During & Miller, 1979). Therefore, a large Vfossa and mmf would imply the presence of a large Vgang and the presence of enhanced face sensitivity, which is only known in semiaquatic taxa (George & Holliday, 2013). In this sense, we infer relative facial sensitivity via trigeminal fossa volume and maxillomandibular foramen maximum diameter (md). We compare endocranial and trigeminal ganglion volumes to data from other taxa, and use the log transformed equation from George and Holliday (2013) relating mmf md and Vfossa volume ($y = 0.2715x + 0.2465$) to discuss the use of both characters when inferring facial sensitivity. We also calculate axon numbers for V_2 and V_3 from the mmf md using the equations relating proximal V_2 axon count and mmf md ($y = 3.7731x + 0.5745$), and proximal V_3 axon count and mmf md ($y = 4.136x + 0.4149$; George & Holliday, 2013).

3 | RESULTS AND DISCUSSION

3.1 | Taphonomic deformation

Taphonomic deformation can significantly alter calculated endocranial volumes. Despite IFSP-VTP/PALEO-0002 and FEF-PV-R-1/9 having similar skull and endocast lengths, they have different endocast volumes, with IFSP-VTP/PALEO-0002 showing only 68% of the values presented by FEF-PV-R-1/9. This result calls for extra attention when reconstructing and evaluating cranial endocasts when only one specimen is available for CT scanning. In this particular case, deformation seems to have occurred in different degrees along the IFSP-VTP/PALEO-0002 endocast. The comparison of PEVs among studied fossil specimens and living representatives of the same clade shows that IFSP-VTP/PALEO-0002 is not uniformly deformed. Whereas rhombencephalic PEV values for this specimen are compatible with the other two adult specimens (111% of FEF-PV-R-1/9 and 96% of FUP-Pv 000020 rhomb PEVs), all other regions have values ranging from 23% to 57% of the values in the other two adult specimens. This makes the rhombencephalic PEV account for more than half of the total endocranial volume (Table 1). In this sense, PEV comparison to related taxa can be used as a proxy for the degree of deformation when only one specimen is available.

In the adult specimens, the dorsoventral deformation is, by far, more evident but despite this, the orientation of the deformation axis does not seem to be the reason for the higher degree of alteration in the calculated volumes.

The juvenile specimen is also dorsoventrally deformed, but its PEV values, as well as calculated relative brain mass, are compatible with the laterally deformed adult specimens (FEF-PV-R-1/9 and FUP-Pv 000020). However, the orientation of the main deformation axis seems to have some impact in the lateral profile of the endocast. In modern crocodilians, the endocasts of specimens representing earlier ontogenetic stages are more dorsoventrally flexed whereas in later ontogenetic stages they are more horizontal (Jirak & Janacek, 2017). This was not the case for the studied specimens, where the juvenile endocast is flatter than the moderately deformed adults are (Figures 2–7). However, disposition of their deformation axes is different. The dorsoventral deformation in the juvenile specimen is bound to have a flattening effect on the endocranial cavity, which would give the endocast a more horizontal profile. Whereas both FEF-PV-R-1/9 and FUP-Pv 000020 were found laying on one of their sides, which implies that any deformation effect would mostly distort/compress the skull laterally. Thus, it seems likely that the generally more horizontal profile of the juvenile is a diagenetic artifact, a feature also found in the dorsoventrally flattened adult specimen IFSP-VTP/PALEO-0002, instead of an ontogenetic process, whereas the flat shape seen in adult specimens can be considered as an actual feature of this taxon and similar to modern crocodilians.

In addition, the juvenile specimen has a markedly arched olfactory region whereas in adult specimens it is either only slightly arched, or not arched at all. In fact, only in the larger adult FUP-Pv 000020, the olfactory region is not arched (Figures 6 and 7). This follows the

TABLE 1 Total endocranial volume (EV) and partial endocranial volume ratios for each brain portion in *Baurusuchus*

		Portion volume ratio			
Specimen	**Total volume (cm^3)**	**Olf**	**Pros**	**Mes**	**Rhomb**
IFSP-VTP/PALEO-0003	5.21	0.20	0.31	0.14	0.35
IFSP-VTP/PALEO-0002	9.85	0.14	0.18	0.16	0.52
FEF-PV-R-1/9	14.51	0.20	0.28	0.20	0.32
FUP-Pv 000020	18.76	0.15	0.42	0.14	0.28
Living Crocodylia along Ontogeny[a]	—	0.05–0.19	0.33–0.56	0.11–0.20	0.25–0.37

Abbreviations: Olf, Olfactory; Pros, prosencephalic; Mes, mesencephalic; Rhomb, rhombencephalic.

[a] Data from Jirak and Janacek (2017).

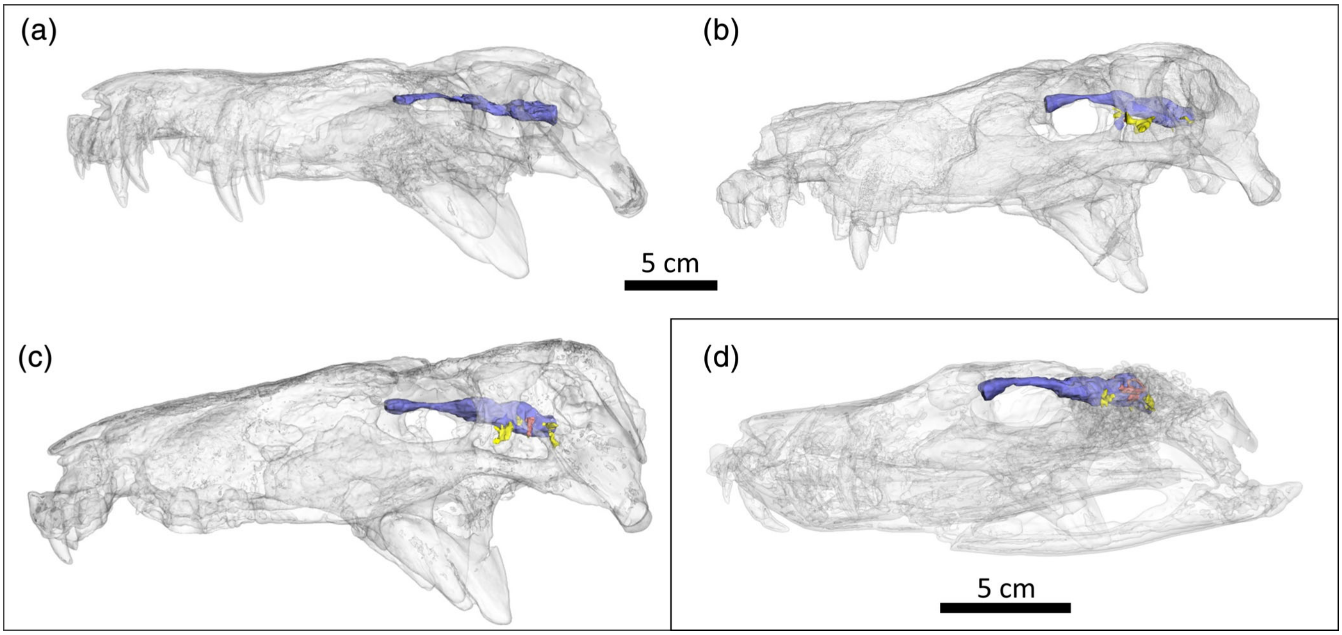

FIGURE 2 Left lateral views of semitransparent skulls with brain endocast reconstructions of studied specimens. IFSP-VTP/PALEO-0002 (a), FEF-PV-R-1/9 (b), FUP-Pv 000020 (c); late juvenile skull right lateral view IFSP-VTP/PALEO-0003 (d). Scale bar: 5 cm

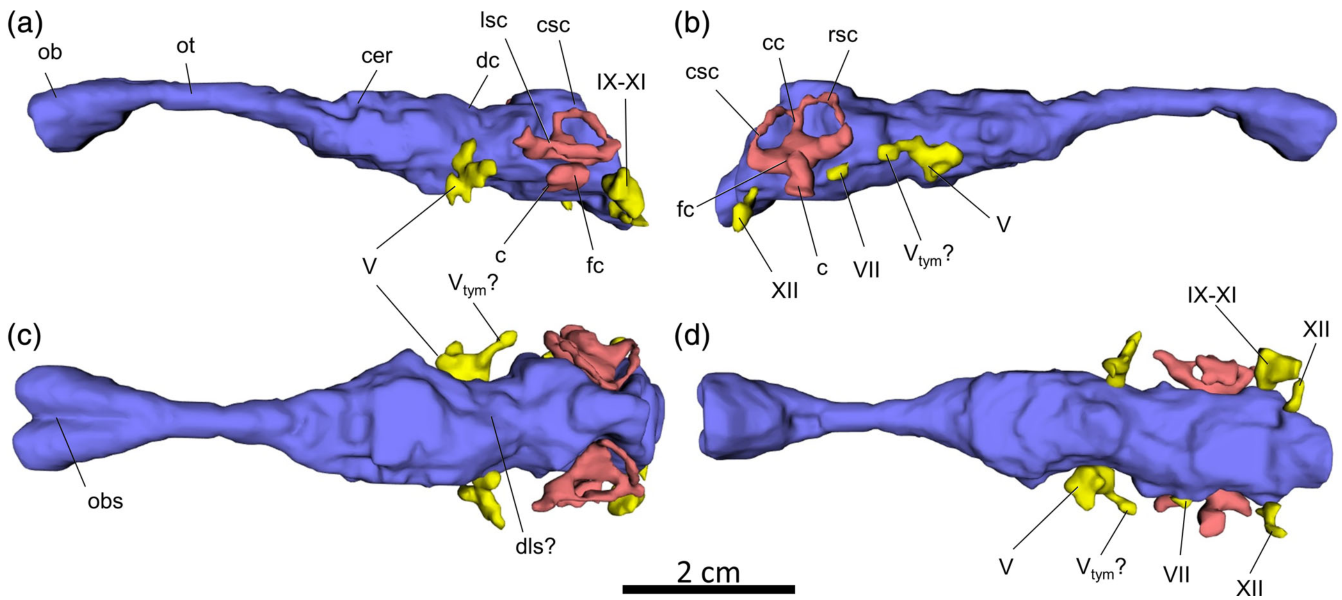

FIGURE 3 Brain endocast, cranial nerves and inner ear of late juvenile specimen IFSP-VTP/PALEO-0003. Left lateral view (a), right lateral view (b), dorsal view (c), ventral view (d). V–XII, cranial nerve canal number; c, cochlea; cc, crus communis; cer, cerebral hemisphere; csc, caudal semicircular canal; dc, dorsal contour; dls, dorsal longitudinal sinus, fc, fenestra cochleae (= round window); lsc, lateral semicircular canal; ob, olfactory bulb; obs, olfactory bulb sulcus; ot, olfactory tract; rsc, rostral semicircular canal; Vtym, tympanic branch of trigeminal nerve canal. Scale bar—2 cm

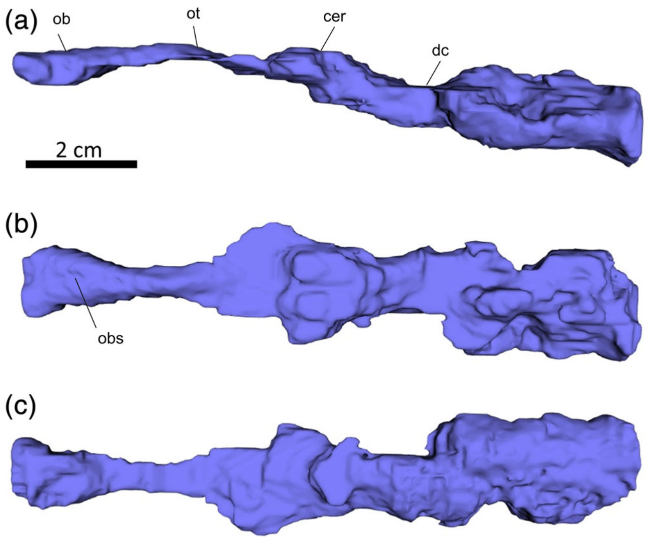

FIGURE 4 Brain endocast of adult specimen IFSP-VTP/PALEO-0002. Left lateral view (a), dorsal view (b), ventral view (c). cer, cerebral hemisphere; dc, dorsal contour; ob, olfactory bulb; obs, olfactory bulb sulcus; ot, olfactory tract. Scale bar—2 cm

pattern found in modern crocodilian ontogeny (Jirak & Janacek, 2017) supporting the idea that *Baurusuchus* brain ontogeny was similar to living Crocodylia and that the flattened lateral profile of the juvenile is more likely to be a diagenetic artifact. This clear difference, along with other characters, might be useful to determine ontogenetic stage in baurusuchid brain endocasts.

3.2 | Brain endocasts and cranial nerves

With exception of a small region below the olfactory tracts, the endocast is completely enclosed in bone, enabling relatively accurate endocranial volume reconstructions. The bones forming the endocranial cavity are the same found in modern Crocodylia. The olfactory bulb region is limited dorsally by the frontal and laterally and ventrally by the prefrontal. The olfactory tract is limited only dorsally and laterally by the frontal. Ventrally, there is no bone enclosing the olfactory tract. The rest of the forebrain is limited dorsally by the parietal, laterally by the laterosphenoid, and ventrally by the basisphenoid. The anterior end of the midbrain is covered dorsally by the parietal and laterally by the laterosphenoid, whereas the posterior end is dorsally and laterally bounded by the prootic. Ventrally, the midbrain is entirely enclosed by the basisphenoid. The anterior region of the hindbrain is enclosed dorsally and laterally by the prootic and ventrally by the basisphenoid. The posterior region of the hindbrain is delimited dorsally and laterally by the exoccipital and ventrally by the basioccipital.

The endocasts are similar in form with exception of IFSP-VTP/PALEO-0002, which has the largest degree of deformation (Figures 3–7). Adult endocast lengths, from the tip of the olfactory bulbs to the end of the medulla oblongata, varies from 111 to 115 mm, whereas the juvenile is approximately 74 mm long. They are largest in

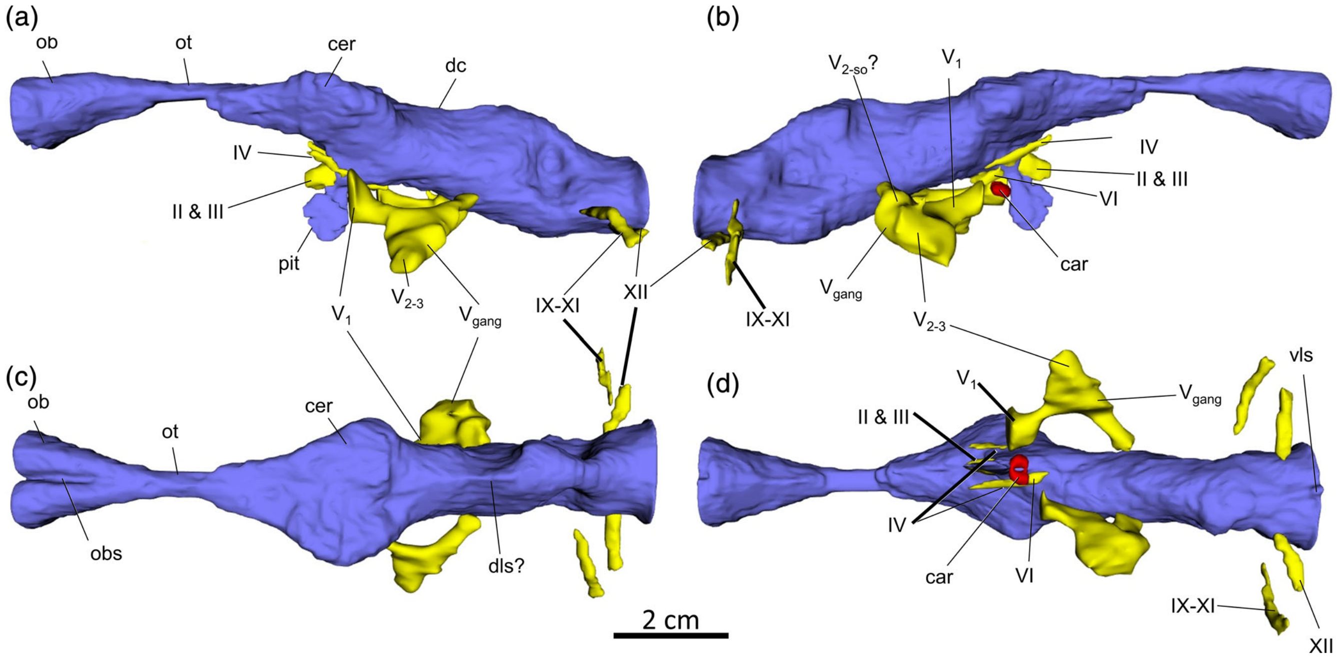

FIGURE 5 Brain endocasts and cranial nerves of adult specimen FEF-PV-R-1/9. Left lateral view (a), right lateral view (b), dorsal view (c), ventral view (d). II—XII, cranial nerve canal number; V1, ophthalmic nerve canal; V2-3, maxillomandibular nerve canal; V2-so, canal for supraorbital branch of maxillary nerve; Vgang, trigeminal (Gasserian) ganglion; car, cerebral carotid artery canal; cer, cerebral hemisphere; dc, dorsal contour; dls, dorsal longitudinal sinus, ob, olfactory bulb; obs, olfactory bulb sulcus; ot, olfactory tract; pit, pituitary gland; vls, ventral longitudinal sinus. Scale bar —2 cm

width at the cerebral hemispheres. Total endocast volumes range from 9.8 to 18.8 cm^3 in the adult specimens and 5.2 cm^3 in the juvenile (Table 1). Reconstructed general endocast morphologies are similar to modern crocodilian endocasts, with different degrees of brain occupancy along the endocranial cavity, with a varying brain-endocast correspondence (Jirak & Janacek, 2017; Watanabe et al., 2019). The correspondent region of the forebrain is more similar to the brain anatomy of living Crocodylia than the midbrain and hindbrain regions. The cerebral and pontine flexures are present but not well developed in the adults, giving the brain endocast a general horizontal, but slightly sigmoid profile, in lateral view. In the juvenile, the flexures are less evident and the endocast is more uniformly horizontal in lateral view, except for the slightly ventrally arched olfactory bulbs.

Partial endocast volumes (PEVs) are close but not completely similar to those of modern Crocodylia (Table 1). The olfactory PEVs fall within or slightly above living Crocodylia values. On the other hand, prosencephalic PEVs are within or below the values for extant Crocodylia, whereas the PEV of IFSP-VTP/PALEO-0002 is remarkably lower, probably due to its higher degree of dorso-ventral deformation in this region. Mesencephalic and rhombencephalic PEVs fall within the modern Crocodylia known limits with exception of the rombencephalic value from IFSP-VTP/PALEO-0002, where its higher value is also likely to be due to its severe deformation in the prosencephalic region.

The olfactory and prosencephalic regions are well marked and easily identifiable, suggesting the brain infilled the endocranial cavity largely in the forebrain portion (olfactory and prosencephalic regions; Figures 3–7). The olfactory bulbs are large and a dorsal longitudinal sulcus, formed by a projection of the frontal, extends along the olfactory bulbs entirely, whereas the olfactory tracts are slender, without any sulcus (Figures 3c, 4b, 5c, and 6b). These conditions are also seen in the juvenile specimen. The combination of the remarkably expanded olfactory bulbs and their dorsal longitudinal sulcus marks the limit between the olfactory bulb and the olfactory tract very clearly. Differently, the limit between olfactory tracts and cerebral hemispheres is not so well marked, mainly because the lateral expansion of the cerebral hemispheres tapers more gradually than the expansion of the olfactory bulbs. However, the anterior limit of the cerebral hemispheres can be located in dorsal view. Posteriorly, the angle between forebrain and midbrain marks the hemispheres limit.

We interpret the relatively high degree of endocast to brain resemblance to be indicative of higher brain to endocranial volumes ratio in the forebrain (Jirak & Janacek, 2017; Watanabe et al., 2019). However, the olfactory region seems to have different degrees of occupation in the olfactory bulbs and tracts, since the resemblance to actual brain anatomy is greater in the olfactory bulb region than the olfactory tract region. Both olfactory bulbs and tracts are separated longitudinally in the actual brain anatomy of living crocodilians (Watanabe et al., 2019), but only the bulbs show signal of separation in *Baurusuchus* endocasts. Unfortunately, the few studies on crocodilian brain and endocranial volumes (BV/EV) neither treated brain/endocast regions separately (Hurlburt et al., 2013; Watanabe et al., 2019), nor treated olfactory bulbs and tracts as separate regions (Jirak & Janacek, 2017). This may be of interest since the olfactory region is the one that reaches the lowest correspondence of BV/EV earlier during ontogeny (Jirak & Janacek, 2017), but in the endocasts reconstructed here, the olfactory bulbs seem to largely occupy the endocranial cavity.

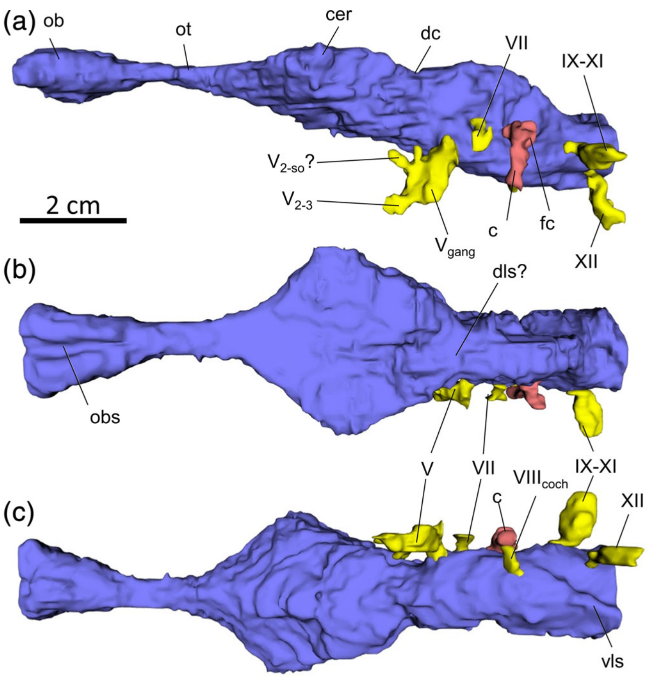

FIGURE 6 Brain endocast, cranial nerves, and inner ear of large adult specimen FUP-Pv 000020. Left lateral view (a), dorsal view (b), ventral view (c). V–XII, cranial nerve canal number; V2-3, maxillomandibular nerve canal; V2-so, canal for supraorbital branch of maxillary nerve; Vgang, trigeminal (Gasserian) ganglion; VIIIcoch, cochlear branch of vestibulocochlear nerve canal; c, cochlea; cer, cerebral hemisphere; dc, dorsal contour; dls, dorsal longitudinal sinus, fc, fenestra cochleae (= round window); ob, olfactory bulb; obs, olfactory bulb sulcus; ot, olfactory tract; vls, ventral longitudinal sinus. Scale bar—2 cm

Olfactory bulbs and tracts have different functions in olfaction: the bulbs are responsible for the initial processing of olfactory signals; the tracts are responsible only for the transmission of those signals to other processing centers in the brain (Mori et al., 1999; Purves et al., 2001). The relative size of a brain region and its function are positively correlated (Bang & Cobb, 1968; Healy & Guilford, 1990; Zelenitsky et al., 2011) so, theoretically, as they have different functions in olfaction, olfactory bulbs and tracts will not necessarily have similar BV/EV ratios. Investigating the BV/EV ratios of olfactory bulbs and tracts separately could potentially refine both total brain volume and olfactory capacity estimations for extinct taxa.

The presence of a sulcus between the olfactory bulbs is not new for crocodyliform endocasts. For instance, it occurs in *C. dinizi* Carvalho et al., 2011, *Notosuchus terrestris* Woodward, 1896, *Sebecus icaeorhinus* Simpson, 1937, *Simosuchus clarki* Buckley et al., 2000, *Uberabasuchus terrificus* Carvalho et al., 2004, and *Wargosuchus australis* Martinelli & Pais, 2008 (Colbert, 1946; Fonseca et al., 2020; Kley et al., 2010; Martinelli & Pais, 2008). This sulcus also might be

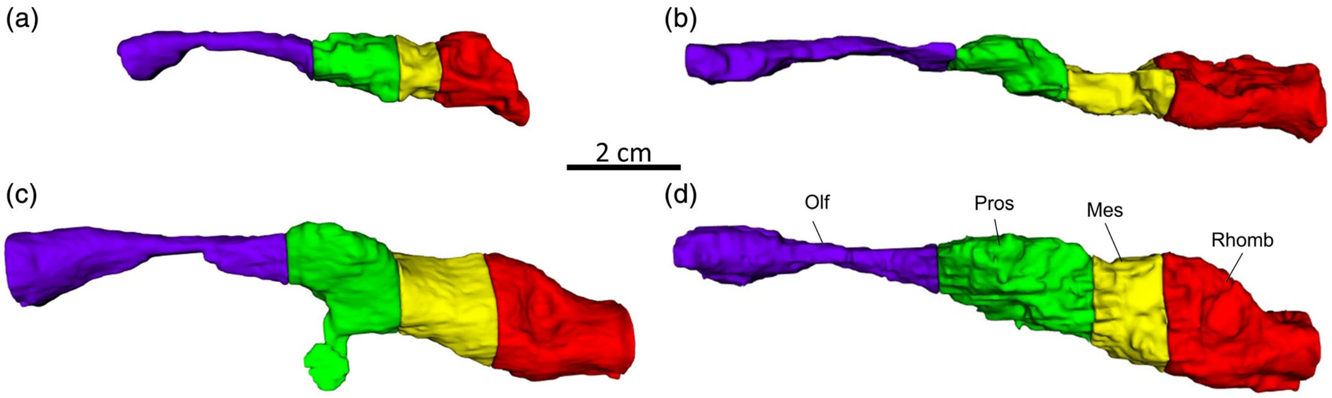

FIGURE 7 Left lateral views of brain endocast reconstructions of studied specimens divided into four major brain sectors. Late juvenile IFSP-VTP/PALEO-0003 (a), adult IFSP-VTP/PALEO-0002 (b), adult FEF-PV-R-1/9 (c), large adult FUP-Pv 000020 (d). Brain portions: olfactory (Olf)—purple, prosencephalic (Pros)—green, mesencephalic (Mes)—yellow, rhombencephalic (Rhomb)—red. Scale bar: 2 cm

present, although shallow, in the peirosaurid *Rukwasuchus yajabalijekundu* (Sertich & O'Connor, 2014) but, unfortunately, part of the olfactory bulbs is missing in the available endocast reconstruction. However, this sulcus seems to be deeper in *Baurusuchus* and *C. dinizi* than in any other available crocodyliform taxa. The sulcus is absent in available modern crocodilian endocasts (Dufeau & Witmer, 2015; Jirak & Janacek, 2017; Witmer et al., 2008). Considering the known distribution of this trait (e.g., present in peirosaurids and baurusuchids but absent in neosuchids), it might be a potentially important phylogenetic character.

Seemingly, the midbrain anatomy is not well defined, probably due to the presence of large dural dorsal venous sinus (Hurlburt et al., 2013; Jirak & Janacek, 2017; Watanabe et al., 2019; Witmer et al., 2008). In dorsal view, the midbrain region becomes mediolaterally narrower posteriorly, evidencing the probable passage of a dorsal longitudinal sinus (dls) (Figures 3c, 5c, and 6b). The narrowing ceases in the hindbrain and the endocasts widen to encase the cerebellum. Posteriorly, the otic capsules compress the endocast mediolaterally without any floccular recess. This evidences either a small or absent flocculus and/or a lower brain volume to endocast volume ratio in the hindbrain than taxa with floccular recess. There is also evidence of a ventral longitudinal sinus (vls), further obscuring hindbrain ventral anatomy (Figures 5d and 6c).

Only in FEF-PV-R-1/9 could the pituitary gland (pit) be reconstructed (Figure 5). It expands ventrally in an elliptical shape without any evident anterior or posterior flexure. Unfortunately, it is laterally deformed and its width cannot be accurately determined. In dorsal view, all endocasts are slightly asymmetric, probably due to fossil diagenetic processes.

In summary, the olfactory bulbs and cerebral hemispheres seem to occupy most of their surrounding endocranial volume, whereas venous sinus or interstitial space largely surrounds the olfactory tracts, midbrain, and hindbrain.

It was also possible to reconstruct the cranial nerves (CN) II, III, IV, V, VI, VII, VIII, IX–XI (via metotic foramen), and XII (Figures 3, 5, and 6). Their position relative to the recognized portions of the endocast is similar to the general pattern of Crocodylomorpha. CN II and III exit the endocranial cavity through the anterior border of the laterosphenoid. It is noteworthy that CN II and III seem to exit the endocranial cavity through a single large opening, instead of CN III having a separate lateral foramen (Figure 5). The foramina for cranial nerves II and III are variable among modern crocodilians. For instance, *Caiman crocodilus* Linnaeus, 1758, *Crocodylus acutus* Cuvier, 1807, *Osteolaemus tetraspis* Cope, 1960, *Tomistoma schlegelii* Müller, 1846, illustrated by Iordansky (1973), do not show a complete separation between CN II and III, although there is a constriction between them. The lack of a distinction between CN II and III might be due to a preservation issue, since this region was only anatomically informative in one of the four *Baurusuchus* specimens herein studied. CN IV passes through the middle portion of the laterosphenoid. CN V is located anterior to the CN VII and cerebellum, with its foramen marking the border between the laterosphenoid and prootic. CN VI exits the endocranial cavity ventrally, through the basisphenoid. CN VII exits anterior to the otic capsule, passing through the prootic. The CN VIII cochlear branch exits below the otic capsule, reaching the endosseous cochlear duct shortly after. The CNs IX-XI exit the endocranial cavity posterior to the otic capsule dorsally, and CN XII is located in the posterior end of the endocranial cavity, more ventrally, with both foramina being located in the exoccipital.

3.3 | Relative brain size

Resulting OLS regression equations from the endocranial cavity and brain volumes were very similar for both groups considered (equation using *A. mississippiensis*: $a = 0.743$, $b = 0.705$; equation using all crocodilians: $a = 0.728$, $b = 0.756$), with high correlation and statistical significance values ($r^2 = .977–0.978$, $p = .0001$; Table 2). Therefore, calculated brain volume from both equations returns similar values regardless of the method or source data (*A. mississippiensis*, "all" crocodilians; Table 3). The results for the PGLS using the "all" crocodilians dataset is identical to the OLS. The only difference is in the value of Akaike Information Criterion, which is slightly better for the PGLS (−51.834) than for the OLS (−49.835).

Brain masses (MBr) calculated using the partial volumes (PV) are almost equal or slightly lower than the ones obtained from the linear regression method (LR, above), with the exception of IFSP-VTP/PALEO-0002 (Table 3), which is considerably lower. In this case, the obtained MBr using PV is only 75% of the value obtained using LR. Estimated body mass ranged from 12.1 kg, for the juvenile individual, to 113.4 kg, for the largest one (see Table 3).

Calculated brain masses were generally similar for both linear regression and partial volumes methods used here. This is probably due to similar partial endocranial volumes by cerebral region among *Baurusuchus* and living crocodilians. However, our results are generally slightly lower when the PEV method is used. Since the BV/EV ratio is not similar for all brain regions (Jirak & Janacek, 2017), further brain volume estimations for

TABLE 2 OLS linear regression equations for log transformed endocranial (EV) and brain volumes (BV) for living crocodilians. For raw data see Supporting Information S1

Taxa	Equation	p	r^2	n (specimens)
Alligator	Log EV = (Log BV × 0.74275) + 0.70453	.0001	.97665	15
Crocodylia	Log EV = (Log BV × 0.7279) + 0.75624	.0001	.97841	20

TABLE 3 Calculated body mass from skull length (equation from Farlow et al., 2005) and brain volumes (BV) from linear equations (Table 2) and partial volumes methods (endocranial volume and ratios in Table 1, model organisms in Jirak & Janacek, 2017) for studied specimens of *Baurusuchus*

		Linear Crocodylia		Linear *Alligator*		Partial volumes	
Specimen	Body mass (kg)	BV, mm^3	BV/EV	BV, mm^3	BV/EV	BV, mm^3	BV/EV
IFSP-VTP/PALEO-0003	12.0	2,897	56%	2,921	56%	2,603	50%
IFSP-VTP/PALEO-0002	72.7	4,603	47%	4,684	48%	3,481	35%
FEF-PV-R-1/9	78.8	6,103	42%	6,246	43%	5,358	37%
FUP-Pv 000020	113.4	7,359	39%	7,560	40%	7,374	39%

fossil reptilian taxa should also investigate if PEVs yield results similar or slightly different from other methods. Traditionally, brain volume estimates for fossil reptilian taxa assume a similar degree of brain to endocast correspondence along different brain regions, and use a series of fixed values of endocranial brain occupancy (e.g., Hurlburt et al., 2013; Knoll & Schwarz-Wings, 2009; Lauters et al., 2013; Paulina-Carabajal & Currie, 2017; Trotteyn & Paulina-Carabajal, 2016; Zhou, Gao, Fox, & Du, 2007). Results achieved in these studies might not be as accurate as if they were to consider different regional BV/EV ratios and a more dynamic BV/EV ratio among different sized specimens.

Plotted log transformed body mass (MBd) and brain mass (MBr) reveals a small relative brain size for *Baurusuchus* when compared to modern crocodilians, even throughout ontogeny (Figure 8). *Baurusuchus* clearly occupies a distinct morphospace in comparison to modern crocodilians. In contrast, living Crocodylia morphospaces are not clearly distinct among species, in all cases their morphospaces overlap with the morphospace of at least one other species. The ontogenetic allometry of *Baurusuchus* seems to have a slope similar to modern crocodilians, but shows a lower intercept (Figure 8). However, the data for *Baurusuchus* is still scarce, with reasonably reliable data for only three individuals, since the brain endocast of IFSP-VTP/PALEO-0002 is highly deformed.

Since encephalization in fossil taxa relies on estimates instead of direct measurements, there is always the possibility that the resulting encephalization estimation is an artifact. As a relative measurement, either an underestimation of MBr or an overestimation of body mass (MBd) would yield an artificially lower encephalization degree. Overestimation of MBd for *Baurusuchus* seems unlikely. Mesoeucrocodylians masses can be estimated by different skeletal measurements, including total length, skull length, and femur length (Farlow et al., 2005). For the almost complete specimens of *Baurusuchus* we used in this study (IFSP-VTP/PALEO-0003 and IFSP-VTP/PALEO-0004) skull length derived MBds yields the lowest values. Underestimation of MBr is more complex. Considering estimated MBds, it would require an MBr at least 20% larger than obtained in order for estimated values for *Baurusuchus* specimens to fall within the lower range of modern crocodilians morphospace. This MBr would represent a BV/EV of 63% in the juvenile specimen and of 47% in the large adult. These values are compatible with the range observed for *A. mississippiensis* (Hurlburt et al., 2013). However, they would still place *Baurusuchus* among the least encephalized crocodyliforms. In order for *Baurusuchus* specimens to have typical modern crocodyliform relative brain sizes, their MBr should be at least 50% higher than estimated values, with BV/EV ratios ranging from 59 to 80%. We cannot completely rule out the possibility that our MBr values are underestimated. However, if they are underestimated, *Baurusuchus* would have much higher BV/EV ratios than modern crocodyliforms and, so far, there is no evidence to support this claim.

3.4 | Olfactory ratio

The olfactory ratio is a measurement of olfactory bulb size relative to cerebral hemisphere size, used to infer olfactory capabilities (Bang & Cobb, 1968; Cobb, 1960; Serrano-Martínez et al., 2019; Zelenitsky et al., 2009, 2011).

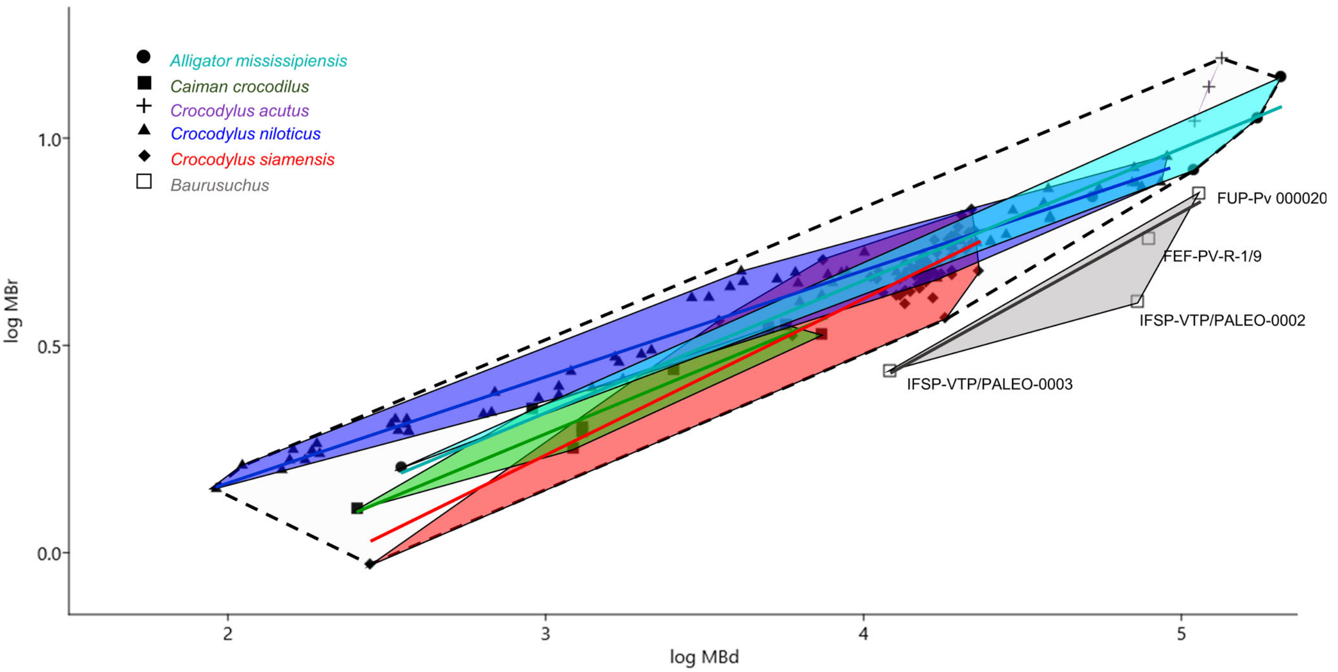

FIGURE 8 Plotted log transformed body and brain mass for crocodyliform taxa with convex hulls morphospace and ontogenetic regression lines. *Alligator mississippiensis*—filled circles, light blue morphospace; *Caiman crocodilus*—filled squares, green morphospace; *Crocodylus acutus*—plus, purple morphospace (no available data for ontogenetic regression); *Crocodylus niloticus*—filled triangles, dark blue morphospace; *Crocodylus siamensis*—filled diamonds, red morphospace; *Baurusuchus*—open squares, yellow morphospace (regression excluding highly deformed specimen); Dashed line—modern Crocodylia morphospace

Reported olfactory ratios for *Alligator mississippiensis* are 49.8, 54.3, and 55.1 for three individuals, being lower in the largest and higher in the smallest measured individuals (Zelenitsky et al., 2009). Therefore, in *Alligator*, the relative volume of the olfactory region decreases as the individual grows. In addition, log transformed olfactory ratios for modern crocodilians range from 1.70 to 1.82 (Serrano-Martínez et al., 2019). These values are considerably lower than the ones found in *Baurusuchus*, which are high and remarkably similar among specimens (raw values ranging from 75.1 to 76.4, log transformed varying from 1.876 to 1.883) and, as far as we could detect, there is no negative allometric relationship for the olfactory ratio in *Baurusuchus*. Deformation does not seem to alter olfactory ratios, probably because the largest measurement of both olfactory bulbs and cerebral hemispheres is their anteroposterior length. However, more intense deformation can preclude locating landmarks for measurements.

Higher olfactory PEV values corroborate the high olfactory ratios, which could support that *Baurusuchus* was more reliant on olfaction than its modern relatives are. However, both olfactory ratios and PEVs are relative measurements. Either a smaller cerebral hemisphere or a larger olfactory bulb would yield higher olfactory ratios and PEVs. Therefore, this discussion would be incomplete without a general relative brain size analysis. Considering the likely lower encephalization degree and the smaller prosencephalic PEVs, it seems that *Baurusuchus* did not have proportionally larger olfactory bulbs, but rather proportionally smaller cerebral hemispheres relative to the olfactory bulbs.

3.5 | Inner ear

Inside the otic capsule lies the inner ear. However, there is not enough contrast in the CT data to reconstruct the complete inner ear anatomy of specimens. The microCT, however, made it possible to reconstruct the inner ear of the fragmented specimen in detail (FUP-Pv 000021; Figure 9). Regular CT scans only allowed partial reconstruction of the inner ear of IFSP-VTP/PALEO-0003 (the juvenile specimen, both left and right) and the left inner ear of FUP-Pv 000020 (Figures 4 and 7). General inner ear morphology is similar to modern Crocodylia, with similar height and semicircular canals placed nearly orthogonally to each other. However, the inner ear is anteroposteriorly shorter than in modern crocodilians, making it slenderer and taller in comparison. This is the ancestral state for crocodyliforms, related to a terrestrial habitat (Schwab et al., 2020). The rostral semicircular canal (rsc) is slightly larger than the caudal semicircular

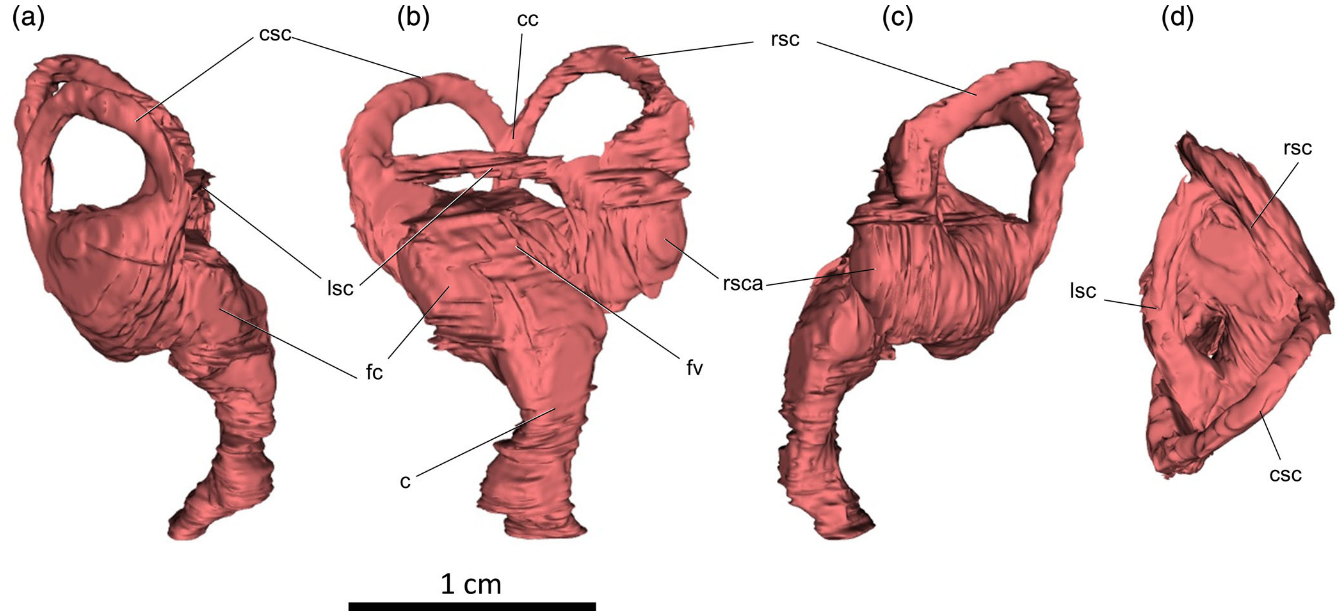

FIGURE 9 FUP-Pv 000021 right inner ear in posterior (a), lateral (b), anterior (c), and dorsal (d) views. Scale bar—1 cm. c, cochlea; cc, crus; fc, fenestra cochleae (= round window); csc, caudal semicircular canal; fv, fenestra vestibuli (= oval window); lsc, lateral semicircular canal; rsc, rostral semicircular canal; rsca, ampulla of rostral semicircular canal

canal (csc), which has the shortest maximum diameter (rsc—8.0 mm, csc—6.3 mm, and lsc—6.7 mm). The lateral semicircular canal (lsc) is also almost orthogonal to the slightly medially arched endosseous cochlear duct (ecd). Reconstructed ecds have similar lengths for FUP-Pv 000020 and FUP-Pv 000021 (9.2 and 10.0 mm, respectively). In IFSP-VTP/PALEO-0003 it is not possible to accurately recover the ecd distal end and its length seems to be slightly longer than what could be measured (4.0 mm). Basicranial axis and ecd scaled/transformed measurements returned a mean best mean hearing of 1,062 Hz, ranging from 283 to 1841 Hz, for FUP-Pv 000020 and of 552 Hz, ranging from 243 to 861 Hz, for IFSP-VTP/PALEO-0003 (Table 4). Calculated mean hearing frequencies and hearing ranges have higher values in the adult probably because we could not accurately calculate ecd length for the juvenile specimen. However, obtained values are compatible with extant crocodilian hearing capabilities (Walsh et al., 2009 and references therein) and with their vocalization frequencies (Vergne, Pritz, & Mathevon, 2009 and references therein). In this sense, *Baurusuchus* hearing and possible vocalizations would be constituted predominantly of mid to low frequencies (<2,000 Hz).

The baurusuchid *C. dinizi* is reported to have a caudal semicircular canal more developed than the rostral semicircular canal (Fonseca et al., 2020) and so far was the only available reconstruction of baurusuchid inner ear. Our reconstructions did not yield the same result, since *Baurusuchus* follows the more common pattern within crocodyliforms, with a rostral semicircular canal larger than the posterior one, as in the notosuchid *Simosuchus clarki* (Kley et al., 2010), modern crocodilians (Brusatte et al., 2016), the noncrocodyliform crocodylomorph *Almadasuchus figarii* Di-Poï & Milinkovitch, 2013 (Leardi, Pol, & Clark, 2020), and most archosaurs (Witmer et al., 2008; Sobral & Müller, 2016). The condition reported for *C. dinizi* is known among Archosauromorpha only in the basal eusuchian *Lohuecosuchus megadontos* (Serrano-Martínez et al., 2019). It is important to note that *C. dinizi* labyrinth reconstruction is actually an estimation, since the authors could not recover the entire extent of semicircular canals due to poor preservation (Fonseca et al., 2020). Considering the close relationship between *Baurusuchus* and *C. dinizi*, the poor preservation of *C. dinizi* inner ear, and the reported condition being rare in crocodyliforms, we advise caution when using the estimated semicircular canals value (as truly having a larger posterior canal than rostral one) in *C. dinizi*. In this sense,

TABLE 4 Best mean hearing and hearing ranges obtained from scaled endosseous cochlear duct for studied specimens (equations in Walsh et al., 2009)

Specimen	Best mean hearing	Hearing range
FUP-Pv 000020	1,062 Hz	283–1841 Hz
IFSP-VTP/PALEO-0003	552 Hz	243–861 Hz

we consider that baurusuchids and closely related forms (e.g., *S. clarki*) are likely to follow the arcosauromorph pattern in having the rsc larger than the csc. Furthermore, the tall and slender inner ear of *Baurusuchus*, with rsc larger than psc is compatible with terrestrial habitat, representing the ancestral state for crocodyliform taxa (Schwab et al., 2020), in contrast to the short looking reconstructed inner ear of *C. dinizi*.

3.6 | Alert head posture

We were not able to reconstruct lateral semicircular canals accurately for the adult specimens with complete skulls to infer alert head posture. However, the almost orthogonal orientation between lsc and endosseous cochlear duct evident in the MicroCT of FUP-Pv 000021 makes it possible to estimate lsc orientation when only ecd anatomy is available. In this sense, alert head posture when lsc is in a complete horizontal position is slightly anteroventrally inclined (Figure 10). When orienting the juvenile IFSP-VTP/PALEO-0003 skull using lsc, the head (skull's long axis) sits at an angle of about 8° anteroventrally in relation to the horizontal plane. The large adult FUP-Pv 000020 provides an inclination of 16°. When using the palate to orient skulls the skull's long axis inclination is the same for lsc in the juvenile (8° anteroventrally), but a little steeper in the large adult (21° anteroventrally), with the lsc 6° anteroventrally inclined. Maxillary tooth row yielded the least steep head inclination, with the skull 3° anteroventrally inclined in the juvenile (with the lsc 5° anterodorsally inclined) and 8° anteroventrally inclined in the large adult (with the lsc 7° anterodorsally inclined). The inferred alert head posture for *Baurusuchus* in all cases is slightly anteroventrally inclined (3°– 8° in the juvenile, 8°–21° in the large adult).

Among the three different methods of inferring alert head posture, our results varied little in the juvenile, with lsc and palate even yielding the same skull angle. The large adult alert head posture varied more but it still had a small variation range (13°). In all cases, approximated lsc angle lies within the known range for archosaurs (Duijm, 1951; Erichsen et al., 1989; Witmer et al., 2003, 2008) and is either aligned to the horizontal plane or slightly inclined (0°–5° anterodorsally in the juvenile, 6° anteroventrally to 7° anterodorsally in the large adult). The similar values obtained by the different methods of inferring alert head posture are concordant with the findings for other notosuchians, as in *Simosuchus clarki*, *C. dinizi*, and *Uberabasuchus terrificus* (Fonseca et al., 2020), as well as for the aetosaur *Neoaetosauroides engaeus* Bonaparte, 1969 (see von Baczko et al., 2018). In *S. clarki*, *C. dinizi*, *U. terrificus*, and *N. engaeus* the difference in alert head posture between palate and lateral semicircular canal methods is of 11°, 10°, 5°, and 3°, respectively (Kley et al., 2010; Fonseca et al., 2020; von Baczko et al., 2018), whereas in *Baurusuchus* there is no difference for the juvenile and a difference of 6° for the large adult. This little to no difference between lsc and palate methods seems to be a trend among terrestrial pseudosuchians. Maxillary tooth row alignment is only available for *N. engaeus* and yielded an antinatural anterodorsal inclination, which is not compatible with

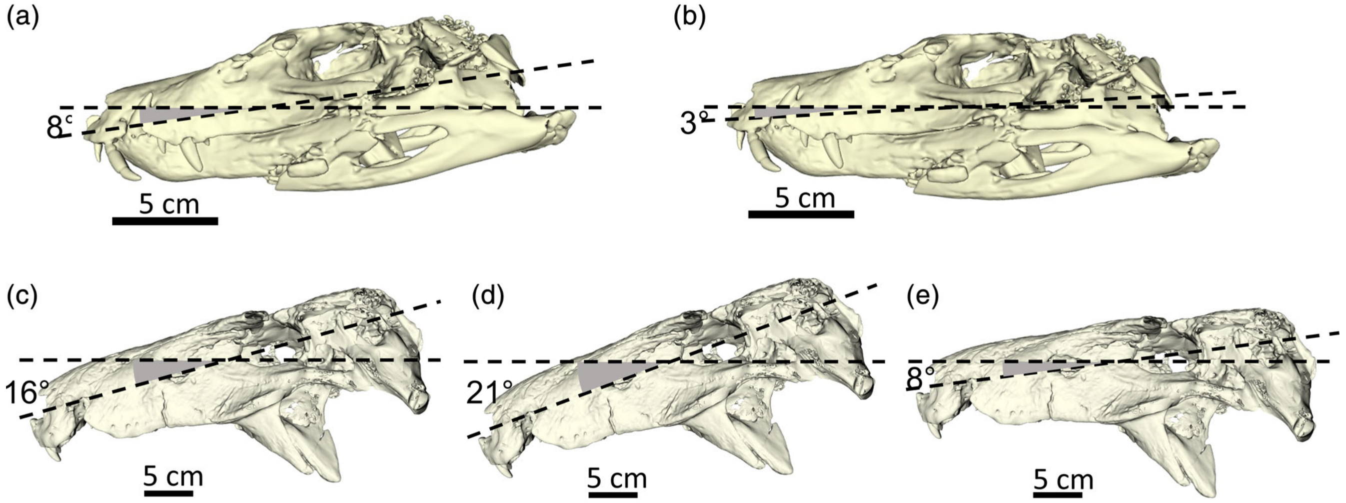

FIGURE 10 Inferred alert head posture aligning the lateral semicircular canal (lsc), palate (pal), and maxillary tooth row (mtr) to the horizontal plane. Late juvenile IFSP-VTP/PALEO-0003 (a—lsc and pal; b—mtr), large adult FUP-Pv 000020 (c—lsc; d—pal; e—mtr). Scale bar—5 cm

the articulation of osteoderms (von Baczko et al., 2018). This contrasts with our results for *Baurusuchus* that were slightly anteroventrally inclined and compatible with head–neck articulation.

It is important to note that Fonseca et al. (2020) present different angles between palate and lateral semicircular canal. Since *C. dinizi* skull sits anteroventrally in a 35° angle when aligned by lsc and in a 25° angle when aligned by the palate, the difference between lsc and palate orientation would be 10°. However, when aligned by the palate, lsc is reported to be 20° inclined in relation to the ground, instead of 10°. The 20° lsc inclination is within known range for archosaurs (Duijm, 1951), despite being much higher than what is inferred for other notosuchids and modern crocodilians, which range from 6° anteroventrally in *Baurusuchus* to 11° anterodorsally in *Simosuchus clarki* (Fonseca et al., 2020; Kley et al., 2010; Witmer et al., 2008). Furthermore, inner ear anatomy of *C. dinizi* is based on a poorly preserved inner ear and the structures in CT reconstruction for *C. dinizi* seem to be misidentified in Fonseca et al. (2020). When estimating lateral semicircular canal anatomy, the authors connected what seems to be part of the ampulla of the rostral semicircular canal to what looks to be the fenestra cochleae (Fonseca et al., 2020 Figure 9). This results in an anteroposteriorly short lsc, that does not meet the base of the caudal semicircular canal and it is much smaller than both other semicircular canals. In comparison, *Baurusuchus*, as well as living crocodilians, has a proportionally longer lsc, which ends near to the base of csc and has the same or larger diameter than csc (Figure 9; Brusatte et al., 2016 Figure 9; Serrano-Martínez et al., 2019 Appendix tables). So far, the anatomy of *C. dinizi* would be unique among mesoeucrocodylians. Therefore, considering the poor preservation of the inner ear of *C. dinizi*, we prefer to consider the *C. dinizi* data as uncertain, as well as its inferred alert head posture using lsc.

Alert head posture in living crocodilians is relatively homogeneous with the skull's long axis held parallel to the horizontal plane (Witmer et al., 2008). The difference found in baurusuchids could be due to different ecologies. Baurusuchids were terrestrial taxa (e.g., Gasparini, Fernandez, & Powell, 1993; Montefeltro et al., 2011; Nascimento & Zaher, 2011; Price, 1945; Riff & Kellner, 2001; Vasconcellos & Carvalho, 2007) whereas modern crocodilians are all semiaquatic (Grigg & Kirshner, 2015). Modern crocodilians often float almost completely submerged, leaving just eyes, nostrils, and ears above water (Grigg & Kirshner, 2015). To hold this position crocodilians must stay with their heads fully horizontally to the water surface, although their bodies are commonly inclined downward (Grigg & Kirshner, 2015). Curiously, the occipital condyle articulation surface is in a similar position in both *Baurusuchus* and modern crocodilians, favoring an inclined articulation between the skull and atlas. It seems that modern crocodilians hold their heads parallel to the horizontal plane with their bodies inclined, whereas baurusuchids held their bodies parallel to the horizontal plane with their heads inclined. Terrestrial taxa, such as baurusuchids, probably would not hold their heads horizontally to the ground, since there is no need to raise sense organs above a certain level. Instead, it is likely that baurusuchids would need their sense organs to be at different heights. In the adult individuals, if the head is parallel to the ground, the nostrils are about six centimeters higher than the height inferred for alert head posture, and sitting farther from the ground, where chemically signaling molecules tend to concentrate (Crimaldi, Wiley, & Koseff, 2002). In addition, holding the head higher is probably energetically costly for terrestrial taxa since it would have to sustain head weight completely without the aid of a water column. Furthermore, the rostrum is narrow near the frontally oriented orbits, but it widens anteriorly, potentially interfering with the visual field and, hypothetically, with stereoscopic vision if the skull's long axis is aligned to the horizontal plane.

The juvenile individual alert head posture is considerably less inclined than the large adult. A few factors may influence this, including head weight, ecological niche occupancy, and the distance between nostrils and the ground. Throughout ontogeny, the cost to maintain a higher alert posture is expected to proportionally increase. There are two reasons for this. The first is that head mass increases at a higher rate than the muscular physiological cross-sectional area of the muscles sustaining head weight, because the latter increases as an area (i.e., to the square), whereas mass increases with volume (i.e., to the cube). The second reason is that the rostrum gets proportionally longer as the individual grows. Both reasons make the head proportionally heavier in relation to the muscular area sustaining the head's weight throughout ontogeny. In addition, it is likely that ecological niches shifted throughout *Baurusuchus* life history, as in modern crocodilians, where hatchlings and juvenile individuals are vulnerable to a wide array of predators whereas adults are often top predators (Grigg & Kirshner, 2015; Somaweera, Brien, & Shine, 2013). Therefore, alert head posture in the juvenile might be related to avoiding predators whereas adults would be only concerned in tracking and hunting for food.

3.7 | Trigeminal fossa and facial sensitivity

A feature regarded as possibly indicative of sensory capacity is the relative size of the trigeminal fossa (George & Holliday, 2013). The relative size of the trigeminal fossa volume in *Baurusuchus*, both with respect to the skull length and to the endocast volume without olfactory tracts and bulbs (as in George & Holliday, 2013), is similar to that of living crocodilians for all three reconstructed adult trigeminal fossa. The Vfossa (mm^3) to skull length (mm) ratio ranges from 0.66 to 1.22 in *Baurusuchus* and 0.34–1.41 in modern crocodilians, and the Vfossa (mm^3) to endocast volume (mm^3) ratio ranges from 1.61 to 3.70% in *Baurusuchus* and 0.67–3.32% in modern crocodilians (Figure 11). The only trigeminal fossa ratio available in literature from a terrestrial taxon is reported for the peirosaurid *Hamadasuchus rebouli* Buffetaut, 1994 (George & Holliday, 2013), which had relatively smaller ones (Vfossa to skull length—0.35; to endocranial volume—1.00%). Therefore, *Baurusuchus* is the only terrestrial crocodyliform taxon with relatively large trigeminal fossa to date.

Before concluding that the large trigeminal fossa in *Baurusuchus* is an indicative of enhanced facial sensation, it is important to remember that the approach by George and Holliday (2013) is a relative measurement of the fossa to the endocranial volume. In this sense, *Baurusuchus* could have a relatively large trigeminal fossa not because of an enhanced facial sensation, but due to a small endocranial volume. As previously discussed, it already seems likely that *Baurusuchus* have had a small relative brain size. This would add to the small endocranial volume hypothesis. In addition, the variable directly linked to axon count number, and therefore facial sensation, is the maxillomandibular foramen maximum diameter (George & Holliday, 2013) and not trigeminal fossa (V fossa) volume. In *Baurusuchus*, the maxillomandibular foramen (mmf) maximum diameter is small in relation to the large trigeminal fossa. The expected mmf maximum diameters from V fossa volume are much higher than the actual measured values in *Baurusuchus* (Table 5). Calculated proximal axon count number for both maxillary (V_2) and mandibular branches (V_3) are much lower than the values for *Alligator mississippiensis* (Table 6). The respective highest calculated axon number values for V_2 and V_3 in *Baurusuchus* are 3,240 and 4,299, whereas the lowest values in *A. mississippiensis* are 11,262 and 26,162 (George & Holliday, 2013).

An enlargement of mmf diameter is directly linked to axon count number, since it makes room for the passage of more axons. The enlargement of the V fossa volumes do not necessarily imply in more room for axon passage

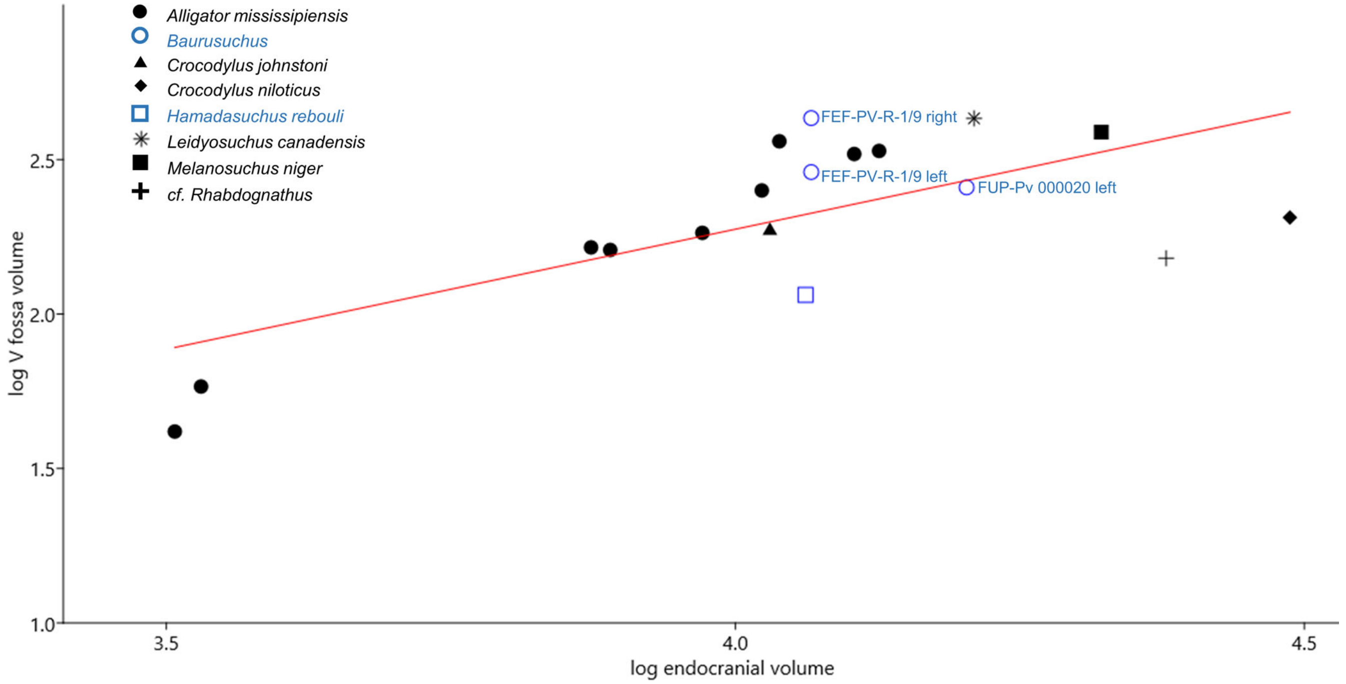

FIGURE 11 Plotted log transformed endocranial volume and trigeminal ganglion volume in several crocodyliform taxa. Black—aquatic/semiaquatic taxa: *Alligator mississippiensis*—filled circles, *Crocodylus johnstoni*—filled triangle, *Crocodylus niloticus*—filled diamond, *Leidyosuchus canadensis*—asterisk, *Melanosuchus niger*—filled square, cf. *Rhabdognathus*—plus. Blue—terrestrial taxa: *Baurusuchus*—open circles, *Hamadasuchus rebouli*—open square

TABLE 5 Measured trigeminal fossa (V fossa) volume and maxillomandibular foramen diameter in *Baurusuchus*, compared to expected maxillomandibular foramen (mmf) diameter from V fossa volume (equation in George & Holliday, 2013)

		mmf maximum diameter (mm)	
Specimen	**V fossa volume (mm^3)**	**Measured**	**Expected**
FEF-PV-R-1/9 right	431	6.0	9.2
FEF-PV-R-1/9 left	288	5.0	8.2
FUP-Pv 000020 left	257	4.7	8.0

TABLE 6 Calculated axon number from maxillomandibular foramen (mmf) maximum diameter for proximal CN V maxillary and mandibular branches (equations in George & Holliday, 2013)

Specimen	Maxillary nerve (V_2)	Mandibular nerve (V_3)
FEF-PV-R-1/9 right	3,240	4,299
FEF-PV-R-1/9 left	1,628	2022
FUP-Pv 000020 left	1,289	1,566
A mississippiensis range[a]	11,262–25,895	26,162–37,289

[a] Data from George and Holliday (2013).

because it would depend on which dimensions of the V fossa are enlarged. If the enlargement of V fossa occurs only longitudinally to the nerve, it would have a larger volume without opening any more room for extra axons. Therefore, we recommend caution in interpreting the large trigeminal fossa as indicative of enhanced facial sensitivity. Although the large V fossa might be a useful phylogenetic character in the future, the mmf maximum diameter is a better proxy for facial sensation.

4 | CONCLUSIONS

When dealing with fossils, the concern about the deformation degree is always present. Here we showed that calculated endocranial volumes from CT scans could be highly affected by taphonomic processes. Comparing partial endocranial volumes with related taxa is a proxy for deformation degree determination in brain endocasts. In addition, dorsoventral flattening precluded any further comment about the ontogenetic stage of a brain endocast. However, the reduction in inclination and arching of the olfactory bulbs through the ontogeny, as is also seen in modern crocodilians, is undoubtedly present in *Baurusuchus*.

Reconstructed *Baurusuchus* endocast morphology is compatible with different degrees of brain occupancy along the endocranial cavity, as reported in the literature. However, there are no sufficiently detailed studies to date to provide accurate information on olfactory region partial brain volume. Apparently, the anatomy of olfactory bulbs and tracts is reflected in different degrees in *Baurusuchus* brain endocasts. Characteristics of brain endocasts might be useful as phylogenetic characters. For example, the presence of a large sulcus between the olfactory bulbs found in *Baurusuchus* is shared with other closely related taxa: baurusuchids (*C. dinizi* and *Wargosuchus australis*), sebecids (*Sebecus icaeorhinus*), and other notosuchians (*Simosuchus clarki, Notosuchus terrestris*, and *Uberabasuchus terrificus*).

Both linear regression and partial volumes methods for calculating brain mass yielded similar results and emerge as potentially more appropriate ways of calculating brain mass in fossil crocodyliforms than using fixed ratios. The allometric relationship of the endocranial cavity and brain was taken in consideration to estimate fossil taxa brain mass, resulting in different BV/EV ratios along ontogeny. Estimated relative brain size revealed that *Baurusuchus* probably had a proportionally smaller brain than modern crocodilians, with smaller cerebral hemispheres. In the light of this information, it seems that the larger olfactory ratio values obtained were not due to larger olfactory bulbs, but due to the smaller cerebral hemispheres and thus we infer no keener sense of smell than in living crocodilians. In order for *Baurusuchus* relative brain size to be similar to that of the living crocodilians, *Baurusuchus* would need to have a much higher BV/EV ratio than living crocodilians do. In summary, either relative brain size or BV/EV ratios were different among *Baurusuchus* and Crocodylia.

Alert head posture for *Baurusuchus* seems to reflect its terrestrial habitat. The slightly anteroventrally inclined head position differs from the horizontal position present in modern day aquatic crocodilians. On the other hand, mean hearing frequencies and hearing ranges values are similar to modern day crocodilians.

In addition, we reported for the first time a terrestrial crocodyliform taxon with a relatively large trigeminal fossa. Despite the link between trigeminal fossa size and facial sensitivity, the large fossa of *Baurusuchus* does not have a compatible maxillomandibular foramen diameter. We recommend caution in interpreting large trigeminal fossae as indicative of enhanced facial sensitivity. For this task, the maxillomandibular foramen maximum diameter is a better proxy. However, the relative size of the trigeminal fossa has potential as an endocranial phylogenetic character.

ACKNOWLEDGMENTS

This study was financed in part by the Coordenação de Aperfeiçoamento de Pessoal de Nível Superior—Brasil (CAPES)—Finance Code 001. The authors also thank CNPq for the grant (401784/2010-0), which supported this research. The authors are in debt to Alexandre Henrique Caetano de Parma (Santa Casa de Votuporanga), Sacha Braun (Nanobiotechnology Laboratory of the Institute of Biology of University of Brasília), Imagens Médicas de Brasília (IMEB) for the CT imaging of the specimens. The authors are grateful to Danilo Furtado for valuable comments on vertebrate neuroanatomy and development of neurosensory system. The authors are also in debt to Casey Holliday and two anonymous reviewers whose comments greatly improved an earlier draft of this MS.

AUTHOR CONTRIBUTIONS

Marcos Dumont Júnior: Conceptualization; formal analysis; investigation; methodology; writing-original draft; writing-review and editing. **Rodrigo Santucci:** Conceptualization; data curation; funding acquisition; investigation; project administration; resources; supervision; writing-review and editing. **Marco Andrade:** Conceptualization; data curation; funding acquisition; resources; writing-review and editing. **Carlos Oliveira:** Conceptualization; data curation; funding acquisition; resources; writing-review and editing.

ORCID

Marcos V. Dumont Jr https://orcid.org/0000-0001-7999-7971

REFERENCES

Akaike H (1973). Information theory and an extension of the maximum likelihood principle. In B. N. Petrov, F. Csáki (Eds.), 2nd International Symposium on Information Theory, Tsahkadsor, Armenia, USSR, September 2–8, 1971, Budapest: Akadémiai Kiadó, pp. 267–281.

Amorim PH, de Moraes TF, Azevedo FDS, da Silva JV. 2011. *InVesalius: Software livre de imagens médicas*. Centro de Tecnologia da Informação Renato Archer-CTI, Campinas/SP-2011-CSBC2011.

Baird, I. L. (1970). The anatomy of the reptilian ear. In C. Gans & T. S. Parsons (Eds.), *Biology of the reptilia, morphology B* (pp. 193–275). New York: Academic Press.

Bang, B. G., & Cobb, S. (1968). The size of the olfactory bulb in 108 species of birds. *The Auk*, *85*, 55–61.

Bapst, D. W. (2012). Paleotree: an R package for paleontological and phylogenetic analyses of evolution. *Methods in Ecology and Evolution*, *3*(5), 803–807.

Bapst, D. W. (2013). A stochastic rate-calibrated method for time-scaling phylogenies of fossil taxa. *Methods in Ecology and Evolution*, *4*(8), 724–733.

Batezelli A. 2003. *Análise da sedimentação cretácea no Triângulo Mineiro e sua correlação com áreas adjacentes*. (PhD dissertation), Universidade Estadual Paulista, Instituto de Geociências e Ciências Exatas. p. 195.

Batezelli, A. (2017). Continental systems tracts of the Brazilian Cretaceous Bauru Basin and their relationship with the tectonic and climatic evolution of South America. *Basin Research*, *29*, 1–25.

Batezelli, A., Saad, A. R., de Jesús Perinotto, J. A., Fulfaro, V. J., & Etchebehere, M. L. D. C. (2003). Análise Estratigráfica aplicada à Formação Araçatuba (Grupo Bauru-Ks) no centro-oeste do Estado de São Paulo. *Geociências*, *22*(1), 5–32.

Benoit, J., Farke, A., Neenan, J., & Manger, P. R. (2019). Is the lateral semicircular canal a reliable proxy to infer head posture? *Journal of Morphology*, *280*, S82–S82.

Blanco, A., Fortuny, J., Vicente, A., Luján, À. H., García-Marçà, J. A., & Sellés, A. G. (2015). A new species of *Allodaposuchus* (Eusuchia, Crocodylia) from the Maastrichtian (Late Cretaceous) of Spain: phylogenetic and paleobiological implications. *PeerJ*, *3*, e1171.

Blanks, R. H. L., Curthoys, I. S., & Markham, C. H. (1972). Planar relationships of semicircular canals in the cat. *American Journal of Physiology-Legacy Content*, *223*, 55–62.

Blumstein, D. T., & Armitage, K. B. (1997). Does sociality drive the evolution of communicative complexity? A comparative test with ground-dwelling sciurid alarm calls. *The American Naturalist*, *150*, 179–200.

Bona, P., Carabajal, A. P., & Gasparini, Z. (2017). Neuroanatomy of *Gryposuchus neogaeus* (Crocodylia, Gavialoidea): A first integral description of the braincase and endocranial morphological variation in extinct and extant gavialoids. *Earth and Environmental Science Transactions of the Royal Society of Edinburgh*, *106*, 235–246.

Bona, P., Degrange, F. J., & Fernández, M. S. (2013). Skull anatomy of the bizarre crocodylian *Mourasuchus nativus* (Alligatoridae, Caimaninae). *The Anatomical Record*, *296*, 227–239.

Brown, C. H., & Waser, P. M. (1984). Hearing and communication in blue monkeys (*Cercopithecus mitis*). *Animal Behaviour*, *32*, 66–75.

Brusatte, S. L., Muir, A., Young, M. T., Walsh, S., Steel, L., & Witmer, L. M. (2016). The braincase and neurosensory anatomy of an Early Jurassic marine crocodylomorph: implications for crocodylian sinus evolution and sensory transitions. *The Anatomical Record*, *299*, 1511–1530.

Buchholtz, E. A., & Seyfarth, E. A. (1999). The gospel of the fossil brain: Tilly Edinger and the science of paleoneurology. *Brain Research Bulletin*, *48*, 351–361.

Buffetaut, E. (1994). A new crocodilian from the Cretaceous of southern Morocco. *Comptes rendus de l'Académie des Sciences*, *319*(12), 1563–1568.

Buschhüter, D., Smitka, M., Puschmann, S., Gerber, J. C., Witt, M., Abolmaali, N. D., & Hummel, T. (2008). Correlation between olfactory bulb volume and olfactory function. *NeuroImage*, *42*, 498–502.

Carvalho, I. S., Gasparini, Z. B., Salgado, L., Vasconcellos, F. M., & Marinho, T. S. (2010). Climate's role in the distribution of the Cretaceous terrestrial Crocodyliformes throughout Gondwana. *Palaeogeography Palaeoclimatology Palaeoecology*, *297*(2), 252–262.

Carvalho, I. S., Teixeira, V. P. A., Ferraz, M. L. F., Ribeiro, L. C. B., Martinelli, A. G., Neto, F. M., … Ferraz, P. F. (2011). Campinasuchus dinizi gen. et sp. nov., a new Late Cretaceous baurusuchid (Crocodyliformes) from the Bauru Basin, Brazil. *Zootaxa*, *2871*, 19–42.

Castro, M. C., Goin, F. J., Ortiz-Jaureguizar, E., Vieytes, E. C., Tsukui, K., Ramezani, J., … Langer, M. C. (2018). A Late Cretaceous mammal from Brazil and the first radioisotopic age for the Bauru Group. *Royal Society Open Science*, *5*(5), 180482.

Chentanez, T., Huggins, S. E., & Chentanez, V. (1983). Allometric relationships for the Siamese crocodile, *Crocodylus siamensis*. *Journal of The Science Society of Thailand*, *9*, 5–26.

Clark, L., Avilova, K. V., & Bean, N. J. (1993). Odor thresholds in passerines. *Comparative Biochemistry and Physiology Part A: Molecular & Integrative Physiology*, *104*, 305–312.

Cobb, S. (1960). Observations on the comparative anatomy of the avian brain. *Perspectives in Biology and Medicine*, *3*, 383–408.

Cohen, B., & Raphan, T. (2004). The physiology of the vestibuloocular reflex (VOR). In S. M. Highstein, R. R. Fay, & A. N. Popper (Eds.), *The vestibular system* (pp. 235–285). New York, NY: Springer.

Cohen, K. M., Finney, S. C., Gibbard, P. L., & Fan, J. X. (2013). The ICS International Chronostratigraphic Chart. *Episodes*, *36*, 199–204.

Colbert, E. H. (1946). *Sebecus*, representative of a peculiar suborder of fossil Crocodylia from Patagonia. *Bulletin of the American Museum of Natural History*, *87*, 2017–2270.

Cotts, L., Pinheiro, A. E. P., Marinho, T. S., Carvalho, I. S., & Di Dario, F. (2017). Postcranial skeleton of *Campinasuchus dinizi* (Crocodyliformes, Baurusuchidae) from the Upper Cretaceous of Brazil, with comments on the ontogeny and ecomorphology of the species. *Cretaceous Research*, *70*, 163–188.

Crile, G., & Quiring, D. P. (1940). A record of the body weight and certain organ and gland weights of 3,690 animals. *The Ohio Journal of Science*, *40*, 219–259.

Crimaldi, J. P., Wiley, M. B., & Koseff, J. R. (2002). The relationship between mean and instantaneous structure in turbulent passive scalar plumes. *Journal of Turbulence*, *3*, 1–24.

Currie, P. J. (1995). New information on the anatomy and relationships of *Dromaeosaurus albertensis* (Dinosauria: Theropoda). *Journal of Vertebrate Paleontology*, *15*, 576–591.

Dendy, A. (1910). On the structure, development, and morphological interpretation of the pineal organs and adjacent parts of the brain in the tuatara (*Sphenudon punctatus*). *Proceedings of the Royal Society of London B*, *82*, 629–637.

Dias-Brito, D., Musacchio, E. A., Castro, J. D., Maranhão, M. S., & Suárez, J. M. (2001). Grupo Bauru: uma unidade continental do Cretáceo no Brasil-concepções baseadas em dados micropaleontológicos, isotópicos e estratigráficos. *Revue de Paleobiologie*, *20*, 245–304.

Di-Poï, N., & Milinkovitch, M. C. (2013). Crocodylians evolved scattered multi-sensory micro-organs. *EvoDevo*, *4*(1), 1–16.

Dufeau, D. L., & Witmer, L. M. (2015). Ontogeny of the middle-ear air-sinus system in *Alligator mississippiensis* (Archosauria: Crocodylia). *PLoS One*, *10*(9), e0137060.

Duijm, M. (1951). On the head posture in birds and its relation to some anatomical features. *Koninklijke Nederlandse Akademie van Wetenschappen.Series C*, *54*, 260–271.

Edinger, T. (1938). Über steinkerne von hirn-und ohr-höhlen der Mesosuchier *Goniopholis* und *Pholidosaurus* aus dem Bückeburger Wealden. *Acta Zoologica*, *19*, 467–505.

Edinger, T. (1941). The brain of *Pterodactylus*. *American Journal of Science*, *239*, 665–682.

Edinger, T. (1975). Paleoneurology 1804-1966. An annotated bibliography (with a foreword by Bryan Patterson). *Advances in Anatomy, Embryology and Cell Biology*, *49*, 1–258.

Endler, J. A. (1992). Signals, signal conditions, and the direction of evolution. *The American Naturalist*, *139*, S125–S153.

Erichsen, J. T., Hodos, W., Evinger, C., Bessette, B. B., & Phillips, S. J. (1989). Head orientation in pigeons: postural, locomotor and visual determinants. *Brain, Behavior and Evolution*, *33*, 268–278.

Evans, L. T. (1936). The development of the cochlea in the gecko, with special reference to the cochlea-lagena ratio and its bearing on vocality and social behavior. *The Anatomical Record*, *64*, 187–201.

Farlow, J. O., Hurlburt, G. R., Elsey, R. M., Britton, A. R., & Langston, W., Jr. (2005). Femoral dimensions and body size of *Alligator mississippiensis*: estimating the size of extinct mesoeucrocodylians. *Journal of Vertebrate Paleontology*, *25*, 354–369.

Felsenstein, J. (2008). Comparative methods with sampling error and within-species variation: contrasts revisited and revised. *The American Naturalist*, *171*(6), 713–725.

Fernandes LA. 1998. *Estratigrafia e evolução geológica da parte oriental da Bacia Bauru (Ks, Brasil). São Paulo*. (PhD Dissertation), Universidade de São Paulo, Instituto de Geociências. p. 272.

Fernandes, L. A., & Coimbra, A. M. (1996). Bacia Bauru (Cretáceo Superior, Brasil). *Anais Acad Bras Cienc*, *68*, 195–206.

Fernandes, L. A., & Coimbra, A. M. (2017). Revisão estratigráfica da parte oriental da Bacia Bauru (Neocretáceo). *Revista Brasileira de Geociencias*, *30*, 717–728.

Fernández, M. S., Carabajal, A. P., Gasparini, Z., & Chong, D. G. (2011). A metriorhynchid crocodyliform braincase from northern Chile. *Journal of Vertebrate Paleontology*, *31*, 369–377.

Fonseca, P. H. M., Martinelli, A. G., Marinho, T. S., Ribeiro, L. C. B., Schultz, C. L., & Soares, M. B. (2020). Morphology of the endocranial cavities of *Campinasuchus dinizi* (Crocodyliformes: Baurusuchidae) from the Upper Cretaceous of Brazil. *Geobios*, *58*, 1–16.

Freckleton, R. P., Harvey, P. H., & Pagel, M. (2002). Phylogenetic analysis and comparative data: a test and review of evidence. *The American Naturalist*, *160*, 712–726.

Gaffney, E. S. (1977). An endocranial cast of the side-necked turtle, *Bothremys*, with a new reconstruction of the palate. *American Museum Novitates*, *2639*, 1–12.

Galton, P. M. (1989). Crania and endocranial casts from ornithopod dinosaurs of the families Dryosauridae and Hypsilophodentidae (Reptilia: Ornithischia). *Geologica et Palaeontologica*, *23*, 217–239.

Galton, P. M. (2001). Endocranial casts of the plated dinosaur *Stegosaurus* (Upper Jurassic, western USA): a complete undistorted cast and the original specimens of Othniel Charles Marsh. In K. Carpenter (Ed.), *The armored dinosaurs* (pp. 103–129). Bloomington, IN: Indiana University Press.

Gans, C. (1980). Allometric changes in the skull and brain of *Caiman crocodilus*. *Journal of Herpetology*, *14*, 297–301.

Garcia, A. J. V., Da Rosa, A. A. S., & Goldberg, K. (2005). Paleoenvironmental and paleoclimatic control on early diagenetic processes and fossil record in Cretaceous continental sandstones of Brazil. *Journal of South American Earth Sciences*, *19*, 243–258.

Garrick, L. D., & Lang, J. W. (1977). Social signals and behaviors of adult alligators and crocodiles. *American Zoologist*, *17*, 225–239.

Gasparini, Z., Fernandez, M., & Powell, J. E. (1993). New tertiary sebecosuchians (Crocodylomorpha) from South America: phylogenetic implications. *Historical Biology*, *7*, 1–19.

George, I. D., & Holliday, C. M. (2013). Trigeminal nerve morphology in *Alligator mississippiensis* and its significance for crocodyliform facial sensation and evolution. *The Anatomical Record*, *296*, 670–680.

Gleich, O., Dooling, R. J., & Manley, G. A. (2005). Audiogram, body mass, and basilar papilla length: correlations in birds and predictions for extinct archosaurs. *Naturwissenschaften*, *92*, 595–598.

Gobbo-Rodrigues, S. R., Petri, S., & Bertini, R. J. (1999). Ocorrências de ostrácodes na Formação Adamantina do Grupo Bauru, Cretáceo Superior da Bacia do Paraná e possibilidades de correlação com depósitos isócronos argentinos. Parte I–Família Ilyocyprididae. *Acta Geologica Leopoldensia*, *23*(49), 3–13.

Godoy, P. L., Montefeltro, F. C., Norell, M. A., & Langer, M. C. (2014). An additional baurusuchid from the Cretaceous of Brazil with evidence of interspecific predation among Crocodyliformes. *PLoS One*, *9*(5), e97138.

Graf, W., De Waele, C., & Vidal, P. P. (1995). Functional anatomy of the head–neck movement system of quadrupedal and bipedal mammals. *Journal of Anatomy*, *186*, 55.

Grafen, A. (1989). The phylogenetic regression. *Philosophical Transactions of the Royal Society B*, *326*, 119–157.

Granot, R., Dyment, J., & Gallet, Y. (2012). Geomagnetic field variability during the Cretaceous Normal Superchron. *Nature Geoscience*, *5*(3), 220–223.

Grap, N. J., Machts, T., Essert, S., & Bleckmann, H. (2020). Stimulus discrimination and surface wave source localization in Crocodilians. *Zoology*, *139*, 125743.

Grigg, G., & Kirshner, D. (2015). *Biology and evolution of crocodylians*, Melbourne: Csiro Publishing.

Groh, S. S., Upchurch, P., Barrett, P. M., & Day, J. J. (2020). The phylogenetic relationships of neosuchian crocodiles and their implications for the convergent evolution of the longirostrine condition. *Zoological Journal of the Linnean Society*, *188*(2), 473–506.

Hammer, Ø., Harper, D. A., & Ryan, P. D. (2001). PAST: paleontological statistics software package for education and data analysis. *Palaeontologia Electronica*, *4*, 9.

Hammock J. 2005. *Structure, function and context: the impact of morphometry and ecology on olfactory sensitivity*. (PhD dissertation), Massachusetts Institute of Technology. p. 308.

Healy, S., & Guilford, T. (1990). Olfactory-bulb size and nocturnality in birds. *Evolution*, *44*, 339–346.

Herrera, Y., Fernández, M. S., & Gasparini, Z. (2013). The snout of *Cricosaurus araucanensis*: a case study in novel anatomy of the nasal region of metriorhynchids. *Lethaia*, *46*, 331–340.

Hoffmann, C. A., Rodrigues, P. G., Soares, M. B., & Andrade, M. B. (2019). Brain endocast of two non-mammaliaform cynodonts from southern Brazil: An ontogenetic and evolutionary approach. *History of Biology*, 1–12. https://www.tandfonline.com/doi/abs/10.1080/08912963.2019.1685512.

Holliday, C. M., & Gardner, N. M. (2012). A new eusuchian crocodyliform with novel cranial integument and its significance for the origin and evolution of Crocodylia. *PLoS One*, *7*, e30471.

Holliday, C. M., & Witmer, L. M. (2009). The epipterygoid of crocodyliforms and its significance for the evolution of the orbitotemporal region of eusuchians. *Journal of Vertebrate Paleontology*, *29*, 715–733.

Hopson, J. A. (1977). Relative brain size and behavior in archosaurian reptiles. *Annual Review of Ecology, Evolution, and Systematics*, *8*, 429–448.

Hopson, J. A. (1979). Paleoneurology. In C. Gans, R. G. Northcutt, & P. Ulinski (Eds.), *Biology of the Reptilia Volume 9: Neurology A* (pp. 39–146). New York, NY: Academic Press.

Hullar, T. E. (2006). Semicircular canal geometry, afferent sensitivity, and animal behavior. *The Anatomical Record*, *288*, 466–472.

Hurlburt GR. 1996. *Relative brain size in recent and fossil amniotes: determination and interpretation*. (PhD dissertation). University of Toronto. p. 253.

Hurlburt, G. R., Ridgely, R. C., & Witmer, L. M. (2013). Relative size of brain and cerebrum in *Tyrannosaurus rex*: An analysis using brain endocast quantitative relationships in extant alligators. In J. M. Parrish, M. Henderson, P. J. Currie, & E. Koppelhus (Eds.), *Origin, systematics, and paleobiology of the tyrannosauridae* (pp. 134–154). Bloomington, IN: Indiana University Press.

Iordansky, N. N. (1973). The skull of the Crocodylia. In C. Gans & T. S. Parsons (Eds.), *Biology of the reptilia: Mophology D* (pp. 201–262). New York, NY: Academic Press.

Jerison, H. J. (1973). *Evolution of the brain and intelligence*. New York, NY: Academic Press.

Jirak, D., & Janacek, J. (2017). Volume of the crocodilian brain and endocast during ontogeny. *PLoS One*, *12*(6), e0178491.

Kley, N. J., Sertich, J. J., Turner, A. H., Krause, D. W., O'Connor, P. M., & Georgi, J. A. (2010). Craniofacial morphology of *Simosuchus clarki* (Crocodyliformes: Notosuchia) from the late Cretaceous of Madagascar. *Journal of Vertebrate Paleontology*, *30*(S1), 13–98.

Knoll, F., & Schwarz-Wings, D. (2009). Palaeoneuroanatomy of *Brachiosaurus*. *Annales de Paleontologie*, *95*, 165–175.

Konishi, M. (1970). Comparative neurophysiological studies of hearing and vocalizations in songbirds. *Journal of Comparative Physiology. A*, *66*, 257–272.

Krebs, J. R., Sherry, D. F., Healy, S. D., Perry, V. H., & Vaccarino, A. L. (1989). Hippocampal specialization of food-storing birds. *Proceedings of the National Academy of Sciences of the United States of America*, *86*, 1388–1392.

Larsson, H. C. E., Sereno, P. C., & Wilson, J. A. (2000). Forebrain enlargement among nonavian theropod dinosaurs. *Journal of Vertebrate Paleontology*, *20*, 615–618.

Larsson, H. C. E., & Sues, H. D. (2007). Cranial osteology and phylogenetic relationships of *Hamadasuchus rebouli* (Crocodyliformes: Mesoeucrocodylia) from the Cretaceous of Morocco. *Zoological Journal of the Linnean Society*, *149*(4), 533–567.

Lauters, P., Vercauteren, M., Bolotsky, Y. L., & Godefroit, P. (2013). Cranial endocast of the lambeosaurine hadrosaurid *Amurosaurus riabinini* from the Amur Region, Russia. *PLoS One*, *8*(11), e78899.

Leardi, J. M., Pol, D., & Clark, J. M. (2020). Braincase anatomy of *Almadasuchus figarii* (Archosauria, Crocodylomorpha) and a review of the cranial pneumaticity in the origins of Crocodylomorpha. *Journal of Anatomy*, *00*, 1–26.

Lefebvre, L., Nicolakakis, N., & Boire, D. (2002). Tools and brains in birds. *Behaviour*, *139*, 939–973.

Leitch, D. B., & Catania, K. C. (2012). Structure, innervation and response properties of integumentary sensory organs in crocodilians. *The Journal of Experimental Biology*, *215*(23), 4217–4230.

Liberona, J. A. P., Soto-Acuña, S., Mendez, M. A., & Vargas, A. O. (2019). Assesment and interpretation of negative forelimb allometry in the evolution of non-avian Theropoda. *Frontiers in Zoology*, *16*(1), 1–13.

Manley, G. A. (1972). A review of some current concepts of the functional evolution of the ear in terrestrial vertebrates. *Evolution*, *26*, 608–621.

Marino, L. (2002). Convergence of complex cognitive abilities in cetaceans and primates. *Brain, Behavior and Evolution*, *59*, 21–32.

Martinelli, A. G., & Pais, D. F. (2008). A new baurusuchid crocodyliform (Archosauria) from the Late Cretaceous of Patagonia (Argentina). *Comptes Rendus Palevol*, *7*, 371–381.

Martins, E. P., & Hansen, T. F. (1997). Phylogenies and the comparative method: a general approach to incorporating phylogenetic information into the analysis of interspecific data. *The American Naturalist*, *149*, 646–667.

Marugán-Lobón, J., Chiappe, L. M., & Farke, A. A. (2013). The variability of inner ear orientation in saurischian dinosaurs: testing the use of semicircular canals as a reference system for comparative anatomy. *PeerJ*, *1*, e124.

Milani, E. J., & Zalan, P. V. (1999). An outline of the geology and petroleum systems of the Paleozoic interior basins of South America. *Episodes*, *22*, 199–205.

Montefeltro, F. C., Larsson, H. C. E., & Langer, M. C. (2011). A new baurusuchid (Crocodyliformes, Mesoeucrocodylia) from the Late Cretaceous of Brazil and the phylogeny of Baurusuchidae. *PLoS One*, *6*(7), e21916.

Mori, K., Nagao, H., & Yoshihara, Y. (1999). The olfactory bulb: Coding and processing of odor molecule information. *Science*, *286*, 711–715.

Narins, P. M., Feng, A. S., Lin, W., Schnitzler, H. U., Denzinger, A., Suthers, R. A., & Xu, C. (2004). Old World frog and bird vocalizations contain prominent ultrasonic harmonics. *The Journal of the Acoustical Society of America*, *115*, 910–913.

Narváez, I., Brochu, C. A., Escaso, F., Pérez-García, A., & Ortega, F. (2015). New crocodyliforms from southwestern europe and definition of a diverse clade of european late cretaceous basal eusuchians. *PLOS ONE*, *10*(11), e0140679.

Nascimento, P. M., & Zaher, H. (2011). The skull of the Upper Cretaceous baurusuchid crocodile *Baurusuchus albertoi* Nascimento & Zaher 2010, and its phylogenetic affinities. *Zoological Journal of the Linnean Society*, *163*(S1), S116–S131.

Newton, E. T. (1888). I. On the skull, brain, and auditory organ of a new species of Pterosaurian (*Scaphognathus purdoni*) from the upper Lias, near Whitby, Yorkshire. *Proceedings of the Royal Society of London*, *43*, 436–440.

Ngwenya, A., Patzke, N., Spocter, M. A., Kruger, J., Dell, L., Chawana, R., … Manger, P. R. (2013). The continuously growing central nervous system of the Nile crocodile (*Crocodylus niloticus*). *The Anatomical Record*, *296*, 1489–1500.

Niimura, Y., & Nei, M. (2006). Evolutionary dynamics of olfactory and other chemosensory receptor genes in vertebrates. *Journal of Human Genetics*, *51*, 505–517.

Nottebohm, F., Kasparian, S., & Pandazis, C. (1981). Brain space for a learned task. *Brain Research*, *213*, 99–109.

O'Brien, H. D., Lynch, L. M., Vliet, K. A., Brueggen, J., Erickson, G. M., & Gignac, P. M. (2019). Crocodylian head width allometry and phylogenetic prediction of body size in extinct crocodyliforms. *Integrative Organismal Biology*, *1*(1), obz006.

Oaks, J. R. (2011). A time-calibrated species tree of Crocodylia reveals a recent radiation of the true crocodiles. *Evolution*, *65* (11), 3285–3297.

Osborn, H. F. (1912). Crania of *Tyrannosaurus* and *Allosaurus*. *Memoirs of the American Museum of Natural History*, *1*, 1–30.

Pagel, M. (1997). Inferring evolutionary processes from phylogenies. *Zoologica Scripta*, *26*, 331–348.

Pagel, M. (1999). Inferring the historical patterns of biological evolution. *Nature*, *401*, 877–884.

Paulina-Carabajal, A., & Currie, P. J. (2017). The braincase of the theropod dinosaur *Murusraptor*: osteology, neuroanatomy and comments on the paleobiological implications of certain endocranial features. *Ameghiniana*, *54*, 617–640.

Pierce, S. E., Williams, M., & Benson, R. B. J. (2017). Virtual reconstruction of the endocranial anatomy of the early Jurassic marine crocodylomorph *Pelagosaurus typus* (Thalattosuchia). *PeerJ*, *5*, e3225.

Platel, R. (1979). Brain weight-body weight relationships. In C. Gans, R. G. Northcutt, & P. Ulinski (Eds.), *Biology of the Reptilia, Neurology A* (Vol. 9, pp. 147–171). New York, NY: Academic Press.

Pol, D., Nascimento, P. M., Carvalho, A. B., Riccomini, C., Pires-Domingues, R. A., & Zaher, H. (2014). A new notosuchian from the Late Cretaceous of Brazil and the phylogeny of advanced notosuchians. *PLoS One*, *9*(4), e93105.

Pol, D., & Powell, J. E. (2011). A new sebecid mesoeucrocodylian from the Rio Loro Formation (Palaeocene) of north-western Argentina. *Zoological Journal of the Linnean Society*, *163*(S1), S7–S36.

Price, L. I. (1945). A new reptile from the Cretaceous of Brazil. *Notas Preliminares e Estudos, Serviço Geologia Mineralogia do Brasil*, *25*, 1–8.

Purves, D., Augustine, G. J., & Fitzpatrick, D. (2001). *Neuroscience*. Sunderland, MA: Sinauer Associates.

Radinsky, L. B. (1968). A new approach to mammalian cranial analysis, illustrated by examples of prosimian primates. *Journal of Morphology*, *124*, 167–180.

Riff, D., & Kellner, A. W. A. (2001). On the dentition of *Baurusuchus pachecoi* price (Crocodyliformes, Metasuchia) from the Upper Cretaceous of Brazil. *Boletim do Museu Nacional, Nova Série, Geologia*, *59*, 1–15.

Riff, D., & Kellner, A. W. A. (2011). Baurusuchid crocodyliforms as theropod mimics: clues from the skull and appendicular morphology of *Stratiotosuchus maxhechti* (Upper Cretaceous of Brazil). *Zoological Journal of the Linnean Society*, *163*(S1), S37–S56.

Rohlf, F. J. (2001). Comparative methods for the analysis of continuous variables: geometric interpretations. *Evolution*, *55*, 2143–2160.

RStudio Team. (2020). *RStudio: integrated development for R Studio*. Boston, MA: PBC http://www.rstudio.com/

Santucci, R. M., & Bertini, R. J. (2001). Distribuição paleogeográfica e biocronológica dos titanossauros (Saurischia, Sauropoda) do Grupo Bauru, Cretáceo Superior do sudeste brasileiro. *Revista Brasileira de Geociencias*, *31*(3), 307–314.

Schwab, J. A., Young, M. T., Neenan, J. M., Walsh, S. A., Lawrence, M., Witmer, L. M., … Brusatte, S. L. (2020). Inner ear sensory system changes as extinct crocodylomorphs transitioned from land to water. *Proceedings of the National Academy of Sciences of the United States of America*, *202002146*, 1–7.

Schwenk, K. (2008). Comparative anatomy and physiology of chemical sense in non-avian aquatic reptiles. In J. G. M. Thewissen & S. Nummels (Eds.), *Sensory evolution on the threshold: Adaptations in secondarily aquatic vertebrates* (pp. 65–81). Berkeley: University of California Press.

Scott, T. P., & Weldon, P. J. (1990). Chemoreception in the feeding behaviour of adult American alligators, *Alligator mississippiensis*. *Animal Behaviour*, *39*, 398–400.

Serrano-Martínez, A., Knoll, F., Narváez, I., Lautenschlager, S., & Ortega, F. (2019). Inner skull cavities of the basal eusuchian *Lohuecosuchus megadontos* (Upper Cretaceous, Spain) and neurosensorial implications. *Cretaceous Research*, *93*, 66–77.

Sertich, J. J., & O'Connor, P. M. (2014). A new crocodyliform from the middle Cretaceous Galula Formation, southwestern Tanzania. *Journal of Vertebrate Paleontology*, *34*, 576–596.

Silva FDP. 2003. *Geologia de subsuperfície e hidroestratigrafia do Grupo Bauru no Estado de São Paulo*. PhD dissertation. Universidade Estadual Paulista, Campus Rio Claro. p. 167.

Soares, D. (2002). An ancient sensory organ in crocodilians. *Nature*, *417*(6886), 241–242.

Soares, P. C., Landim, P. M., Fúlfaro, V. J., & Neto, A. F. S. (1980). Ensaio de caracterização estratigráfica do Cretáceo no estado de São Paulo: Grupo Bauru. *Brazilian Journal of Geology*, *10*, 77–185.

Sobral, G., & Müller, J. (2016). Archosaurs and their kin: the ruling reptiles. In J. A. Clack, R. R. Fay, & A. N. Popper (Eds.), *Evolution of the vertebrate ear. Evidence from the fossil record* (pp. 285–326). Cham: Springer.

Somaweera, R., Brien, M., & Shine, R. (2013). The role of predation in shaping crocodilian natural history. *Herpetological Monographs*, *27*, 23–51.

Spoor, F. (2003). The semicircular canal system and locomotor behaviour, with special reference to hominin evolution. *Cour Forschungsinst Senckenberg*, *243*, 93–104.

Spoor, F., Garland, T., Krovitz, G., Ryan, T. M., Silcox, M. T., & Walker, A. (2007). The primate semicircular canal system and locomotion. *Proceedings of the National Academy of Sciences of the United States of America*, *104*, 10808–10812.

Spoor, F., & Zonneveld, F. (1998). Comparative review of the human bony labyrinth. *American Journal of Physical Anthropology*, *107*(S27), 211–251.

Steiger, S. S., Fidler, A. E., Valcu, M., & Kempenaers, B. (2008). Avian olfactory receptor gene repertoires: Evidence for a well-developed sense of smell in birds? *Proceedings of the Royal Society of London B*, *275*, 2309–2317.

Stensiö, E. A. (1963). The brain and cranial nerves in fossil lower craniate vertebrates. *Skrifter utgitt av Det Norske Videnskaps-Akademi i Oslo*, *13*, 1–120.

Tamrat, E., Ernesto, M., Fulfaro, V. J., Saad, A. R., Batezelli, A., & Oliveira, A. F. (2002). Magnetoestratigrafia das formações Uberaba e Marília (Grupo Bauru) no Triângulo Mineiro (MG). *Simpósio sobre o Cretáceo do Brasil*, *6*, 323–327.

Taylor, M. P., Wedel, M. J., & Naish, D. (2009). Head and neck posture in sauropod dinosaurs inferred from extant animals. *Acta Palaeontologica Polonica*, *54*, 213–220.

Trotteyn, M. J., & Paulina-Carabajal, A. (2016). Braincase and neuroanatomy of *Pseudochampsa ischigualastensis* and *Tropidosuchus romeri* (Archosauriformes, Proterochampsia). *Ameghiniana*, *53*, 527–543.

Turner, A. H., & Calvo, J. O. (2005). A new sebecosuchian crocodyliform from the Late Cretaceous of Patagonia. *Journal of Vertebrate Paleontology*, *25*(1), 87–98.

Tykoski, R. S., Rowe, T. B., Ketcham, R. A., & Colbert, M. W. (2002). Calsoyasuchus valliceps, a new crocodyliform from the Early Jurassic Kayenta Formation of Arizona. *Journal of Vertebrate Paleontology*, *22*, 593–611.

Vasconcellos, F. M., & Carvalho, I. S. (2007). Cranial features of *Baurusuchus salgadoensis* Carvalho, Nobre & Campos, 2005, a Baurusuchidae (Mesoeucrocodylia) from the Adamantina Formation, Bauru Basin, Brazil: Paleoichnological, taxonomic and systematic implications. In I. D. S. Carvalho, A. C. S. Fernandes, M. A. C. Rodrigues, M. S. S. Carvalho, M. Arai, & M. E. Q. Oliveira (Eds.), *Paleontologia: Cenários de Vida* (pp. 240–327). Rio de Janeiro: Interciência.

Vasconcellos FM, Marinho TS, Carvalho IS. 2007. The locomotion pattern of *Baurusuchus salgadoensis* Carvalho, Nobre and Campos, 2005 and the distribution of Baurusuchidae in Gondwanaland: *XII Gondwana, Abstracts*. p. 363.

Vassar, R., Chao, S. K., Sitcheran, R., Nun, J. M., Vosshall, L. B., & Axel, R. (1994). Topographic organization of sensory projections to the olfactory bulb. *Cell*, *79*, 981–991.

Vergne, A. L., Pritz, M. B., & Mathevon, N. (2009). Acoustic communication in crocodilians: from behaviour to brain. *Biological Reviews*, *84*, 391–411.

von Baczko, M. B., Taborda, J. R., & Desojo, J. B. (2018). Paleoneuroanatomy of the aetosaur *Neoaetosauroides engaeus* (Archosauria: Pseudosuchia) and its paleobiological implications among archosauriforms. *PeerJ*, *6*, e5456.

von During, M. (1973). The ultrastructure of lamellated mechanoreceptors in the skin of reptiles. *Anatomy and Embryology*, *143*, 81–94.

von During M. 1974. The ultrastructure of the cutaneous receptors in the skin of *Caiman crocodilus*. *VS Verlag für Sozialwissenschaften, Wiesbaden*, *53*, 123–134.

von During, M., & Miller, M. R. (1979). Sensory nerve endings in the skin and deeper structures. In C. Gans, R. G. Northcutt, & P. Ulinski (Eds.), *Biology of the reptilia, 9. Neurology A* (pp. 407–442). New York: Academic Press.

Walsh, S. A., Barrett, P. M., Milner, A. C., Manley, G., & Witmer, L. M. (2009). Inner ear anatomy is a proxy for deducing auditory capability and behaviour in reptiles and birds. *Proceedings of the Royal Society B*, *276*, 1355–1360.

Walsh, S. A., & Knoll, M. A. (2011). Directions in palaeoneurology. *Special Papers in Palaeontology*, *86*, 263–279.

Watanabe, A., Gignac, P. M., Balanoff, A. M., Green, T. L., Kley, N. J., & Norell, M. A. (2019). Are endocasts good proxies for brain size and shape in archosaurs throughout ontogeny? *Journal of Anatomy*, *234*, 291–305.

Weldon, P. J., & Ferguson, M. W. J. (1993). Chemoreception in crocodilians: Anatomy, natural history and empirical results. *Brain, Behavior and Evolution*, *41*, 239–245.

Wenzel, B. M., & Meisami, E. (1987). Number, size, and density of mitral cells in the olfactory bulbs of the northern fulmar and rock dove. *Annals of the New York Academy of Sciences*, *510*, 700–702.

Wilson JA, Malkani MS, Gingerich PD. 2001. New crocodyliform (Reptilia, Mesoeucrocodylia) from the Upper Cretaceous Pab Formation of Vitakri, Balochistan (Pakistan). *Contributions from Paleontolqgy—University of Michigan*, *30*(12), 321–336.

Witmer, L. M., Chatterjee, S., Franzosa, J., & Rowe, T. (2003). Neuroanatomy of flying reptiles and implications for flight, posture and behaviour. *Nature*, *425*, 950–953.

Witmer, L. M., Ridgely, R. C., Dufeau, D. L., & Semones, M. C. (2008). Using CT to peer into the past: 3D visualization of the brain and ear regions of birds, crocodiles, and nonavian dinosaurs. In H. Endo & R. Frey (Eds.), *Anatomical imaging* (pp. 67–87). Tokyo: Springer.

Zelenitsky, D. K., Therrien, F., & Kobayashi, Y. (2009). Olfactory acuity in theropods: palaeobiological and evolutionary implications. *Proceedings of the Royal Society B*, *276*, 667–673.

Zelenitsky, D. K., Therrien, F., Ridgely, R. C., McGee, A. R., & Witmer, L. M. (2011). Evolution of olfaction in non-avian theropod dinosaurs and birds. *Proceedings of the Royal Society B*, *278*, 3625–3634.

Zhou, C. F., Gao, K. Q., Fox, R. C., & Du, X. K. (2007). Endocranial morphology of *Psittacosaurs* (Dinosauria: Ceratopsia) based on CT scans of new fossils from the Lower Cretaceous, China. *Palaeoworld*, *16*, 285–293.

SUPPORTING INFORMATION

Additional supporting information may be found online in the Supporting Information section at the end of this article.

How to cite this article: Dumont Jr MV, Santucci RM, de Andrade MB, de Oliveira CEM. Paleoneurology of *Baurusuchus* (Crocodyliformes: Baurusuchidae), ontogenetic variation, brain size, and sensorial implications. *Anat Rec*. 2020;1–25. https://doi.org/10.1002/ar.24567